Biogeographic responses and niche occupancy of microbial communities following long-term land-use change

Dennis Goss-Souza (dennisgoss10@gmail.com)
Universidade do Estado de Santa Catarina Centro de Ciências Agroveterinárias https://orcid.org/0000-0003-3362-1789

Siu Mui Tsai
University of São Paulo

Jorge Luiz Mazza Rodrigues
University of California at Davis

Osmar Klauberg-Filho
Santa Catarina State University

José Paulo Sousa
University of Coimbra

Dilmar Baretta
Santa Catarina State University

Lucas William Mendes
University of São Paulo

Research Article

Keywords: Biodiversity hotspots, historical contingency, land-use change, microbial distance-decay, microbial niche specialization, soil bacterial co-occurrence

Posted Date: January 20th, 2022

DOI: https://doi.org/10.21203/rs.3.rs-1250532/v1

Biogeographic responses and niche occupancy of microbial communities following long-term land-use change

Dennis Goss-Souza[1,2,3*], Siu Mui Tsai[1], Jorge Luiz Mazza Rodrigues[2,4], Osmar Klauberg-Filho[3], José Paulo Sousa[5], Dilmar Baretta[3,6], Lucas William Mendes[1]

[1]Center for Nuclear Energy in Agriculture, University of São Paulo, Piracicaba, SP, 13400-970, Brazil
[2]Department of Land, Air and Water Resources, University of California at Davis, Davis, CA 95616, USA
[3]Department of Soils and Natural Resources, Santa Catarina State University, Lages, SC 88523-000, Brazil. Current professional address
[4]Environmental Genomics and Systems Biology Division, Lawrence Berkeley National Laboratory, Berkeley, CA, 94720, USA
[5]Department of Life Sciences, University of Coimbra, Coimbra, Coimbra, P3000-456, Portugal.
[6]Department of Soils and Sustainability, Santa Catarina State University, Chapecó, SC, 89815-630, Brazil.

***Corresponding author:** Santa Catarina State University - UDESC
Department of Soils and Natural Resources
Soil Ecology and Ecotoxicology Laboratory
Av. Luis de Camões, 2090
Lages, SC, 88523-000
Brazil
Phone: +55-49-3289-9233
E-mail: dennis.souza@udesc.br

Dennis Goss-Souza, http://orcid.org/0000-0003-3362-1789

Siu Mui Tsai, http://orcid.org/0000-0002-3733-6312

Jorge Luiz Mazza Rodrigues, http://orcid.org/0000-0002-6446-6462

Osmar Klauberg-Filho, http://orcid.org/0000-0002-7733-9745

José Paulo Sousa, http://orcid.org/0000-0001-8045-4296

Dilmar Baretta, http://orcid.org/0000-0001-8219-1362

Lucas William Mendes, http://orcid.org/0000-0003-0980-7006

Funding information. This study was funded by the São Paulo Research Foundation (FAPESP/CNPq No. 2008/58114-3 and FAPESP/NSF No. 2014/50320-4) and by the National Council for Scientific and Technological Development (SisBiota-CNPq No.

563251/2010-7). DG-S received a scholarship from CNPq-FAPESP (PRONEX-CNPq/FAPESP No. 140317/ 2014-7). DB thanks CNPq for his Research Productivity Grant (CNPq-PQ No. 305939/2018-1). SMT also thanks CNPq for her Research Productivity Grant (CNPq-PQ No. 311008/2016-0). LWM thanks FAPESP for his Young Researcher Grant (FAPESP No. 2020/12890-4 and 2019/16043-7). We thank all the staff of the SisBiota Thematic Project, for helping us in sampling campaigns and soil analyses.

Ethical statement. This article does not contain any studies with human participants and/or animals performed by any authors.

Consent to participate. Not applicable.

Consent for publication. Not applicable.

Data availability. All data generated or analyzed in this study are included in the article and its supplementary information files.

Conflict of interest. The authors declare that they have no conflict of interest.

Author contributions. DG-S, SMT, OK-F, JPS, and DB, designed the project. DG-S, OK-F, and DB collected the soil samples. DG-S and LWM performed molecular biology analyses. DG-S, LWM, and JLMR analyzed the data. All authors wrote, commented, and accepted the final version of the manuscript.

Abstract

Understanding the effects of forest-to-agriculture conversion on microbial diversity has been a major goal in soil ecological studies. However, linking community assembly to the ruling ecological processes at local and regional scales remains challenging. Here, we evaluated bacterial community assembly patterns and the ecological processes governing niche specialization in a gradient of geography, seasonality, and land-use change, totalizing 324 soil samples, 43 habitat characteristics (abiotic factors), and 16 metabolic and co-occurrence patterns (biotic factors), in the Brazilian Atlantic Rainforest, a subtropical biome recognized as one the world's largest and most threatened hotspots of biodiversity. We observed no significant shifts in alpha diversity due to land-use change. Meanwhile, pairwise beta diversities and distance decays were lower in pastures than those observed for forest and no-till soils. Pasture communities showed a predominantly neutral model, regarding stochastic processes, with moderate dispersion, leading to biotic homogenization. Most no-till and forest microbial communities followed a niche-based model, with low rates of dispersal and weak homogenizing selection, indicating niche specialization or variable selection. Historical and evolutionary contingencies, as represented by soil type, season, and dispersal process were the main drivers of microbial assembly and processes at the local scale, markedly correlated with the occurrence of endemic microbes. Our results indicate that the patterns of assembly and their governing processes are dependent on the niche occupancy of the taxa evaluated (generalists or specialists). They are also more correlated with historical/evolutionary contingencies and the interactions among taxa (i.e. co-occurrence patterns) than the land-use change itself.

Keywords: Biodiversity hotspots, historical contingency, land-use change, microbial distance-decay, microbial niche specialization, soil bacterial co-occurrence.

Introduction

The Brazilian Atlantic Forest is the fourth world's richest hotspot of biodiversity, harboring 2.7% and 2.1% of the global endemic species of plants and vertebrates, respectively (Myers et al. 2000). However, in recent decades this biome has suffered from extensive fragmentation and destruction of forest canopies, with only 11.7% of the original vegetation remaining (Ribeiro et al. 2009). The conversion of forests to both croplands and pasturelands represents 20 and 42% of the total human net primary production (HNPP) appropriation in this biome (Weinzettel et al. 2018). By 2100, land-use change is expected to reduce natural vegetative cover by 26-58% in all 34 global hotspots of biodiversity, compared to 2005 (Jantz et al. 2015). The same study predicted that, by the end of the century, forest conversion to croplands and pasturelands could contribute up to 1/3 of the habitat loss and up to 16% loss of plant and animal species in those hotspots due to land-use change only.

As with plants and animals, soil microorganisms are very responsive to land-use change (Lauber et al. 2013; Kaiser et al. 2016; Li et al. 2019; Ceola et al. 2021). Investigations of local microbial communities in the Amazon Forest Biome (Northwestern Brazil) have shown that the conversion of forest in pasturelands and croplands often leads to bacterial diversity loss (Jesus et al. 2009; Rodrigues et al. 2013; Mendes et al. 2015b; Goss-Souza et al. 2020) and affects ecosystem services related to the microbial activity (Paula et al. 2014; Meyer et al. 2017; Goss-Souza et al. 2019; Pedrinho et al. 2019). Most of the works listed above have described taxa trade-offs, diversity turnover, and shifts in microbial functions, resulting from land-use change, as dependent on local abiotic environmental filters (e.g. soil pH, soil organic matter, soil fertility), which is indicative of homogeneous selection process (Stegen et al. 2013). When looking to the Atlantic Forest, just a few works evaluated the diversity of soil

bacterial communities in the subtropical region of this biome (Southern Brazil) (Faoro et al. 2010) and the consequences of forest-to-agriculture conversion for both bacterial diversity and ecological processes shaping bacterial distribution (Goss-Souza et al. 2017).

The hypothesis of distance-decay relationship (DDR) of biodiversity, which infers about the decrease of taxa similarity (or increase in taxa dissimilarity) the extend the distance between pairwise microbial communities increase has been applied with success to solve this ecological gap (Horner-Devine et al. 2004; Martiny et al. 2011; Shade et al. 2018; Gao et al. 2019). Complementary to the DDR, the continuum hypothesis states that stochastic processes along with deterministic selection contribute to the assembly of ecological communities (Stegen et al. 2013; Dini-Andreote et al. 2015; Powell et al. 2015; Tripathi et al. 2018). DDRs have been linked with success with the ecological dispersal process (Martiny et al. 2011), which refers to the tendency to migrate by individuals from a local population or community, leading to homogenous dispersal, when rates of migration are high or, dispersal limitation, when the dispersal rates are low (Sengupta et al. 2019). The variation in microbial diversity related to random birth and death or spatial distance between sites, not related to environmental selection, indicates a drift process. Drift could act as the dominant process in microbial communities when overall population abundance and community diversities are low (Nemergut et al. 2013), leading to an increased risk of extinction (Cordovez et al. 2019). Moreover, dispersal and drift can act together as stochastic forces, leading to microbial neutral assembly (Cottenie 2005; Székely and Langenheder 2014; Goss-Souza et al. 2017, 2020).

The homogeneous selection is assumed to be a pivotal driver of local assembly dynamics of bacterial communities (e.g. in the same toposequence) (Jesus et al. 2009; Dini-Andreote et al. 2014; Mendes et al. 2015a). However, several studies have shown weak correlations between assembly and homogeneous environmental filtering in

regional or continental scales (Feng et al. 2019; Gao et al. 2019). The explanation could reside in a complementary selection force, the variable selection process, which occurs when heterogeneous selective environments lead microbial communities to be overdispersed (e.g. increase in SOM quantity and/or quality, microbial cooperation and co-occurrence, microbial activity) (Dini-Andreote et al. 2015), with microbial communities modulated by intra- and interspecific biotic relationships among species, in detriment of environmental abiotic filters (Gao et al. 2019). To account for this, species association has been regularly used in microbial ecology to infer biotic interactions resulting from the variable selection process (Ferrenberg et al. 2013; Nemergut et al. 2013; Wang et al. 2020). Otherwise, just a few studies have used microbial networks for examining species association and variable selection in biogeographical studies (Ma et al. 2016; Gao et al. 2019). The outcome of network topological properties results in co-occurrence and co-exclusion patterns, which can offer valuable insights about biotic interactions within sets of microbial communities (Dini-Andreote et al. 2014; Jones and Hallin 2019), although some studies have argued that spatial associations between species is not a good proxy for ecological interactions (Blanchet et al. 2020). Microbial ecologists are now focusing on the hypothesis that, besides homogeneous selection, other ecological processes, such as variable selection, dispersal limitation, and drift are important drivers of the variability in assembly patterns along with geographic gradients (Hanson et al. 2012; Ranjard et al. 2013). However, a few studies have tested and quantified those complementary processes in biogeography studies (Fan et al. 2017; Feng et al. 2019; Gao et al. 2019).

As soil microbial communities are often very complex, most biogeography studies have described the distance decay patterns in terms of overall communities (Martiny et al. 2011; Ranjard et al. 2013; Rodrigues et al. 2013). However, a few recent studies have

raised the hypothesis that the distance decay relationship and, consequently, the ecological processes governing assembly in bacterial communities could vary between habitat generalists and specialists (Gao et al. 2019; Luo et al. 2019). While generalists follow the Baas Becking theory of "everything is everywhere" (De Wit and Bouvier 2006), habitat specialists are the microorganisms that have restricted occupancy, as represented by their low occurrence across environmental and geographical gradients (Meyer et al. 2018; Gao et al. 2019; Ceola et al. 2021). The competitive/cooperative interactions among microbial populations in a local community (Li et al. 2018) and sets of metapopulations in metacommunity (Hovatter et al. 2011; Rocha et al. 2021) are very intricate (Leibold et al. 2004) and land-use change can greatly alter the role of these interactions in microbial community assembly (Creamer et al. 2016; Brinkmann et al. 2019; Goss-Souza et al. 2020). Some authors have found land-use change and management intensification in tropical soils, as selective abiotic filters, by increasing the competition among species for habitat and limiting resources, according to niche (Mendes et al. 2014; Goss-Souza et al. 2019). Linking the occurrence of those endemic and ubiquitous taxa with the environmental and geographical gradients could enable microbial ecologists to survey the consequences of human intervention on microbial diversity and habitat specialization. Furthermore, it will allow us to depict the possible relationships between aboveground plant habitat and diversity loss, due to deforestation and land-use change and the outcome for belowground soil microbial communities, with consequences for management and conservation strategies in this threatened biome.

Here, we investigated the distribution and DDR patterns of beta diversities and consequent ecological processes governing microbial assembly along with multiple spatial scales. Moreover, we linked those patterns and processes to habitat transformation, resulting from the long-term conversion of the Atlantic Forest into no-till cropping and

pasture areas. Our central hypothesis affirmed that (i) the microbial assembly would vary along land uses, and geographic distance between microbial communities with a decrease in microbial diversity in the converted agriculture soils of local communities. We also hypothesized that (ii) the balance between neutral and niche-based assembly models would differ along land uses and spatial scales, being neutral in the forest soils, and local communities and niche-based in the agriculture soils and regional communities. A third hypothesis stated that (iii) the processes governing microbial assembly would vary from stochastic to deterministic between habitat generalists and specialists, respectively. By combining 16S rRNA T-RFLP fingerprint and a large set of abiotic (43 soil and landscape parameters) and biotic factors (16 metabolic and co-occurrence patterns) in a broad spatial scale (0-378 km), we aimed (i) to verify the changes in bacterial assembly patterns, (ii) to identify the features that impose assembly, and (iii) to underlie the ecological processes governing assembly across spatial scales for overall bacterial communities, generalists and specialists.

Material and Methods

Study areas, soil sampling, and environmental analyses

The sampling sites were located within the subtropical Atlantic Forest Biome, at Santa Catarina State, Brazil (Supplementary Fig. S1a), and represented (1) remnants of the original forest cover, and the long-term conversion of forest into (2) no-till cropping and (3) pasturelands. The forest sites comprised a natural transition between mixed ombrophilous forest and semi-deciduous forest, with a predominance of *Araucaria angustifolia* (fam. Araucariaceae) in the western mesoregion and *Mimosa scabrella* (Fabaceae) in the plateau mesoregion. Other frequent species in forest sites were *Apuleia leiocarpa*, *Balfourodendron riedelianum*, *Cabralea glaberrima*, *Cedrela fissilis*, *Cordia*

210 *trichotoma*, *Diatenopterix sorbifolia*, *Enterolobium contortisiliquum*, *Lonchocarpus*
211 *leucanthus*, *Parapiptadenia rigida*, *Patagonula americana,* and *Peltophorum dubium*.
212 Forest areas were deforested via timber slash-and-burn and converted in two distinct land
213 uses, in the late 1980s: i) No-till cropping systems, characterized by successive rotational
214 cultivation of wheat, and eventually, oat and ryegrass in the winter, followed by soybean
215 and maize in the summer, and; ii) Pasturelands, characterized by a mix of perennial
216 grasses with a predominance of *Axonopus affinis* (Poaceae) in western mesoregion and
217 *Andropogon lateralis* (Poaceae) in plateau mesoregion. The selection of sampling sites
218 was based on land-use history and management, obtained from previous exploratory
219 campaigns, interviewing farmers and experts. The main criterion of selection was the
220 conversion of forest to no-till or pasture at least 10 years before sampling. Samples were
221 collected in July and January, comprising winter and summer seasons of the southern
222 hemisphere, respectively, in a gradient of latitude, longitude, and altitude. Sampling
223 counties were São Miguel do Oeste (26°44'S; 53°32'W; 652 meters above sea level -
224 masl), Chapecó (27°3'S; 52°40'W; 642 masl) and Xanxerê (26°50'S; 52°28'W; 728
225 masl) in the western mesoregion and, Campo Belo do Sul (27°52'S; 50°39'W; 978 masl),
226 Lages (27°47'S; 50°35'W; 877 masl) and Otacílio Costa (27°33'S; 49°52'W; 902 masl),
227 in the Plateau mesoregion, Santa Catarina State, Brazil (Supplementary Fig. S1a). The
228 climate in both mesoregions is humid temperate mesothermal (Cfb) (Köppen
229 classification), with no marked dry season and rainfalls equally distributed throughout the
230 year. The historic mean annual temperature varies from 18–22°C in the western to 14–
231 18°C in the Plateau.

232 To evaluate microbial assembly patterns (response variables), non-deformed soil
233 samples from the 0–10 cm profile were collected with sterile PVC tubes (5 cm diameter
234 × 10 cm depth), yielding ~ 500 g of soil each. Each sample was collected in a 3 × 3

Cartesian square-geogrid scheme, equidistantly by 30 m from each other, with 20 m of the border, totalizing an area of one hectare per sampling site (Supplementary Fig. S1b). A total of 324 individual soil samples were collected (9 samples per geogrid × 3 land uses × 6 counties × 2 sampling seasons). Samples were kept on dry ice and transported to the Cell and Molecular Biology Laboratory, Center for Nuclear Energy in Agriculture (Piracicaba, Brazil), within 24 hours, to further molecular procedures. For soil physical, chemical, and microbiological parameters, used as explanatory variables, samples were collected at the same points (also totalizing 324 independent samples). Soil samples were maintained at 4°C and transported to the Soil Analysis Laboratory, Santa Catarina State University (Lages, Brazil). The soil physical analyses performed were soil density, porosity (total-, macro-, micro- and bioporosity), texture, particle density, aggregate diameter, and penetration resistance. The chemical characteristics analyzed were soil pH, total C, H, N, and S, C:N ratio, soil organic matter, soil organic C, P, K, Al, Ca, and Mg. All the physical and chemical analyses were performed following routine methodology (Keeney and Nelson 1982; Gee and Bauder 1986; Dexter 1988; Cambardella and Elliott 1992; Tedesco et al. 1995; Claessen et al. 1997; Dexter et al. 2007; Dhaliwal et al. 2011; Teixeira et al. 2017). Microbiological metabolic analyses included soil microbial C, soil basal respiration, metabolic quotient, and microbial quotient, also performed through a routine methodology (Sparling and West 1988; Sparling 1992; Anderson and Domsch 1993; Alef and Nannipieri 1995). Soil types were classified using the World Reference Base for Soil Resources (Anjos et al. 2015). Details about site management history, sampling, and environmental analyses are available as supporting information. See also (Bartz et al. 2014; Goss-Souza et al. 2017).

Soil total DNA extraction and 16S rRNA T-RFLP

To investigate bacterial diversity patterns and processes structuring bacterial communities across land uses, seasons, and geographical distances, we used the T-RFLP method. T-RFLP quantifies the variability in DNA sequences of genes or intergenic space regions (e.g. bacterial small subunit 16S rRNA, fungal ITS), generating a DNA 'fingerprint' of unique fragments, with the size and abundance of each fragment in a soil sample. Although sequencing provides more detailed phylogenetic information, T-RFLP as an automated fingerprinting method is a simpler and less expensive system that allows the comparison of a high amount of soil samples (van Dorst et al. 2014), with sufficient replication to address soil microbial patterns of diversity and structure (Fierer and Jackson 2006; Dumbrell et al. 2010; Székely and Langenheder 2014; Lange et al. 2015; Kari et al. 2019). Also, T-RFLP generates results consistent with that found in high throughput sequencing (Vega-Avila et al. 2014; Powell et al. 2015; Durrer et al. 2017; Karczewski et al. 2017; De Vrieze et al. 2018). To accomplish that, total DNA extraction (250 mg) was performed for the 324 soil samples (See Supplementary Fig. S1), using PowerLyzer PowerSoil™ DNA Isolation Kit (Mo Bio Laboratories, Carlsbad, USA). DNA quality was verified in gel electrophoresis with Tris-buffered saline with sodium boric acid and 1% agarose (Brody and Kern 2004). DNA concentration was measured with the Qubit™ fluorometer (Thermo Fischer Scientific, Waltham, USA). T-RFLP fragments amplification was performed in a thermal cycler GeneAmp PCR System 9700™ (Thermo Fischer Scientific, Waltham, USA), using the 16S rRNA universal set of primers 27F (5' AGA GTT TGA TCC TGG CTC AG 3') labeled with 6-FAM (Edwards et al. 1989) and 1492R (5' GGT TAC CTT GTT ACG ACT T 3') (Turner et al. 1999). The PCR mix contained 10X Platinum Taq PCR buffer, 3.0 mM $MgCl_2$, 0.2 mM of each dNTP, 0.5 mM of each primer and 0.05 U μL^{-1} of Platinum™ Taq DNA polymerase (Thermo Fischer Scientific, Waltham, USA). DNA templates (10-50 ng μL^{-1}) were ten-fold diluted to

285 optimize the reaction. Reaction consisted in a pre-denaturation step at 94°C for 3 minutes,
286 followed by 35 cycles of 94°C for 30 seconds, 59°C for 45 seconds, and 72°C for 60
287 seconds, with a final extension of 72°C for 15 minutes. Reaction products were then
288 purified using GFX^{TM} PCR DNA and Gel Band Purification Kit (GE Health Care,
289 Chicago, USA), according to the manufacturer's instructions. Ten to 60 nanograms of the
290 amplified and purified DNA were used in 10 µl of restriction reaction using *Hha*I
291 endonuclease (Thermo Fischer Scientific, Waltham, USA), at 37°C for 3 hours. Digested
292 DNA was then purified using 60 µl of absolute ethanol with 2 µl of sodium acetate/EDTA
293 (100:1; 0.1%) and centrifuged at 4000 × *g* for 45 minutes, followed by another step,
294 adding 150 µl of absolute ethanol/water (7:3) and centrifuging at 4000 × *g* for 45 minutes.
295 The purified DNA pellet was eluted in 9.8 µl of deionized formamide with 0.2 µl of
296 GeneScan-500 ROX^{TM} internal size standard (Thermo Fischer Scientific, Waltham,
297 USA). The product was denatured at 94°C for 5 minutes in a thermal cycler GeneAmp
298 PCR System 9700^{TM} (Thermo Fischer Scientific, Waltham, USA). Fragments were
299 analyzed in an ABI Prism 3100^{TM} automated sequencer (Thermo Fischer Scientific,
300 Waltham, USA) following the manufacturer's instructions. The size and the intensity of
301 each terminal restriction fragment were estimated using GeneMapper version 3.0
302 (Thermo Fischer Scientific, Waltham, USA) and are hereafter described in terms of
303 operational taxonomic units (OTUs) (Schütte et al. 2008; Rodríguez-Valdecantos et al.
304 2017). Only fragments ranging from 50 to 500 bp were analyzed.
305
306 **Microbial profiling and assembly patterns**
307 We first calculated the overall Chao-1 estimated richness and Shannon's alpha diversity
308 for each land use and season. Means were compared through ANOVA with Tukey's
309 Honest Significant Difference test (Tukey's HSD), with the function 'tukeyHSD', on R

310 software, version 4.0.2 (R Core Team, 2020). To evaluate the overall distribution of beta
311 diversities, we performed a multivariate Principal Coordinates Analysis (PCoA), with
312 Monte-Carlo permutations on Canoco software, version 5.2 (Lepš and Šmilauer 2005).
313 From the resulting Bray-Curtis distance matrix, we measured the clustering of beta
314 diversities resulting from PCoA ordination, through non-parametric Permutational
315 Analysis of Variance (PERMANOVA), as implemented by 'adonis' function in 'vegan'
316 package, version 2.5-6 (Anderson 2001; Oksanen et al. 2019), on R software. Adonis-
317 PERMANOVA allowed us to test whether beta diversities were separated by land use,
318 season, and geographic location. Then, we calculated the distributions of observed beta
319 Sørensen pairwise dissimilarities, using the function 'beta.pair' in 'betapart' R package,
320 version 1.5.1 (Baselga et al. 2018). We partitioned the values Sørensen pairwise beta
321 diversities (B_{SOR}) into the turnover (B_{SIM}) and the nestedness (B_{SNE}) components of
322 diversity. We found that the turnover component dominated the partitioning for all land-
323 uses and seasons (Supplementary Fig. S2). Moreover, using Sørensen's presence/absence
324 matrices and analyzing samples from a large geographic scale (0-378 km) in the same
325 dataset, pairwise comparisons almost reached the limit of the signal of the Sørensen index
326 ($B_{SOR} = 1$) for all land uses and seasons. Thus, we decided to depict the variation in
327 diversification through pairwise Bray-Curtis abundance-based dissimilarities, across land
328 uses and seasons, using the function 'beta.multi.abund' (Baselga 2017), also in the
329 'betapart' R package. We performed the Shapiro-Wilk W test for normal probability,
330 using the function 'shapiro.test' on R. Data presented non-parametric distribution, hence
331 we used the Kruskal-Wallis (chi-square) non-parametric test, with corrected P-values to
332 compare the means of beta diversities across land uses and seasons, using the function
333 'kruskal.test' on R.
334

335 **Microbial co-occurrence patterns**

336 To obtain a signal of microbial ecological interactions modulating assembly complexity
337 patterns, we performed non-random co-occurrence network analysis, using the Python
338 'SparCC' tool, which estimates correlation values from compositional data (Friedman
339 and Alm 2012). First, we calculated SparCC co-occurrence metrics for overall
340 communities, according to land use and season (54 samples × 3 land uses × 2 seasons =
341 324 samples). Complementary, pairwise microbial communities were compiled in local
342 and regional communities, within and over the mesoregion threshold, respectively,
343 according to spatial distance. Local and regional communities were defined by
344 complementary analyses of Moran's I test for spatial autocorrelation and 3D spatial
345 interpolation through the gridding semivariogram method, with Jackknife cross-validate
346 permutations. After defining the limit distance for autocorrelation, we calculated SparCC
347 co-occurrence metrics for local communities, which is the set of pairwise communities
348 within Moran's threshold for autocorrelation and regional communities, regarded as the
349 pairs of microbial communities over the limit for autocorrelation. For each network
350 (overall, local or regional), P-values were obtained by 100 random permutations for each
351 set of samples. Only OTUs with SparCC significant ($P < 0.01$) and correlations with a
352 magnitude of SparCC > 0.6 or < -0.6 were included into the network analyses. The nodes
353 in the reconstructed networks represented the OTUs, while the edges represented
354 significant positive or negative correlations between nodes. Co-occurrence patterns were
355 calculated in the interactive platform Gephi, version 0.9.2 (Bastian et al. 2009), and
356 network graphs were built with the 'Fruchterman Reingold' design. The metrics evaluated
357 were average node connectivity, average path length, cumulative degree distribution,
358 network diameter modularity, number of edges, number of nodes, and number of
359 communities. The resulting values of those metrics were used as biotic factors,

representing the variable selection process, on further multivariate partitioning analyses. From the resulting networks, we were also able to extract the major hub taxa, represented by the set of OTUs with the highest betweenness centrality, which measures the extent to which a node lies on paths between other nodes.

To test the turnover of microbial abundances across land uses and seasons, we performed the Multinomial Species Classification Method (CLAM test) (Chazdon et al. 2011), classifying all the possible phylotypes (275 OTUs) according to their habitat specialization, as generalists and specialists, using the 'clamtest' function, in 'vegan' R package, according to the estimated species relative abundance. The test was applied using the supermajority rule ($K = 2/3$, $P < 0.005$). After that, we were able to investigate whether the hub OTUs in each network were generalists or specialists.

Distance-decay patterns of beta diversities

To assess the geographic scale dependence of microbial community diversities, we performed distance-decay relationship (DDR) models of beta pairwise Bray-Curtis dissimilarities, ranging from 0.03 to 378 km (See map, Supplementary Fig. S1a), using the function 'decay.model', in the 'vegan' R package (Nekola and Mcgill 2014; Gómez-Rodríguez and Baselga 2018). The best-fitted GLM model was chosen according to the lowest Akaike Information Criterion (AIC) value (Gómez-Rodríguez and Baselga 2018) and the highest pseudo-R^2 value (Robeson et al. 2011). After choosing the best-fitted model, we used the slope (the rate at which dissimilarity increases with distance), associated with a p-value, to infer the significance of the best-fitted decay model.

Assembly models, selection, and dispersal

384 To investigate the species association patterns across land uses and seasons, we calculated
385 species rank abundance distributions (RADs) for each of the 324 samples and fitted them
386 to four different theoretical assembly models: the zero-sum multinomial (ZSM) and the
387 broken stick (null model), which regard to neutral assembly, and; the pre-emption and the
388 log-normal, related to a niche-based assembly. Broken stick, pre-emption and, log-normal
389 models were calculated using the 'radfit' function from the 'vegan' R package. The ZSM
390 model was calculated on TeTame software, version 2.16 (Jabot et al. 2008). The models
391 were compared based on the AIC. The lowest AIC value, the best-fitted model for each
392 sample (Bozdogan 1987). The dispersal rates, related to the tendency to migrate from
393 members of a certain community, were calculated for each sample, through Etienne's
394 formula (Etienne and Alonso 2005), on TeTame.

395 From the Bray-Curtis dissimilarity matrices, we calculated beta-diversity
396 distributions for local and regional communities with the function 'vegdist' on the 'vegan'
397 R package (Oksanen et al. 2019). Then, we performed permutations resemblance of those
398 Bray-Curtis dissimilarity distance distributions under the null model with the function
399 'swap_count' from the 'vegan' R package. Afterward, we generated the Z-scores for the
400 set of microbial communities with the function 'oecsimu' (Ulrich and Gotelli 2010), also
401 from the 'vegan' R Package. The Z-score refers to the deviation of expected Bray-Curtis
402 pairwise distributions under permutations to the observed value, indicating the distance
403 of a certain set of pairwise beta diversities from the null expectation (Keil 2019). Pairwise
404 diversities with Z-score < -2 reflected aggregation, which means that OTUs co-occurred
405 more than expected by the null model, while pairwise diversities with Z-score > +2
406 reflected segregation, meaning that OTUs co-occurred less than expected by the null
407 model (Dini-Andreote et al. 2015; Gao et al. 2019). We considered the co-occurrence
408 patterns of microbial communities as non-random, resulting from deterministic

409 homogeneous (Z-score < -2) or variable selection (Z-score > +2) processes, while Z-
410 scores within those values (-2 < Z-score < +2), indicated that communities co-occurred
411 randomly, governed by drift and/or dispersal stochastic processes.
412
413 **Variation partitioning of factors modulating assembly of microbial communities**
414 To investigate the importance of geographic coordinates as primary predictors of Bray-
415 Curtis dissimilarities across spatial scales, we first performed a Principal Coordinates
416 Analysis of Neighbor Matrices (PCNM), with forward-selection, setting Latitude,
417 longitude, and altitude as primary predictors and the resulting coordinates (PCNM axes)
418 as spatial predictors. Latitude and longitude were used as constraining variables in the
419 model. From the resulting PCNM non-collinear and significant variables (Bonferroni
420 correction), we depicted the proportion of the variation in the microbial assembly of
421 overall bacterial communities, generalists and, specialists explained by (1) geography, (2)
422 abiotic factors, and (3) biotic factors, via Mantel and partial Mantel tests, with Pearson
423 correlations, according to geographic distance, with the functions 'mantel' and
424 'partial.mantel' (Legendre and Fortin 1989), in the 'vegan' R Package.
425
426 **Results**
427 **Profiling of microbial communities**
428 Chao-1 Richness and Shannon's α-diversity (*H'*) among land uses and seasons were
429 compared through Tukey's HSD test (Supplementary Fig. S3). Richness of OTUs did not
430 vary across land uses in winter season (P_{same} = 0.414). Otherwise, we found differences
431 in richness for summer (P_{same} = 0.018), with no-till (Chao-1 = 92.3±21.7) richer than
432 pasture (Chao-1 = 79.1±27.8) (P = 0.027), and no differences between forest (Chao-1 =
433 80.5±28.9) and no-till (P = 0.055) or forest and pasture (P = 0.960). When comparing

seasons within the same land use, we found no differences between winter and summer richness for forest (P = 0.175) and pasture (P = 0.892), with samples from no-till summer (Chao-1 = 92.3±21.7) richer than winter (Chao-1 = 80.0±30.7; P = 0.018). The same patterns were observed for α-diversity, which did not vary across land uses in the winter (P_{same} = 0.540) and varied across land uses in summer (P_{same} < 0.001). Depicting the variability in summer, no-till presented higher α-diversity (*H'* = 3.8±0.4) when compared to both forest (*H'* = 3.5±0.4; P = 0.004) and pasture (*H'* = 3.2±0.4; P < 0.001), with forest α-diversity higher than pasture (P < 0.001). Comparing seasons within the same land use, we found no differences between winter and summer α-diversity for forest (P = 0.250) and pasture (P = 0.114), with samples from no-till summer (*H'* = 3.8±0.4) more diverse than winter (*H'* = 3.4±0.7; P = 0.003).

Beta diversity structures and distributions

We investigated the beta diversity structure among land uses, through PCoA. The plot based on Bray-Curtis distances showed differences in structures of no-till microbial communities with both forest and pasture communities. Otherwise, forest and pasture communities presented a high degree of overlapping (Fig. 1). Variation in Bray-Curtis distances explained in the first two axes of PCoA was 34.78%. Depicting the clustering of beta diversities resulting from principal coordinates ordination we found differences among land uses (PERMANOVA, Pseudo-F = 4.65, P = 0.008), seasons (Pseudo-F = 7.51, P = 0.007) and sampling sites, represented by the six different counties (Pseudo-F = 12.08, P < 0.001). Thus, to explore the first two significant correlations from PERMANOVA, we depicted the variation in beta pairwise diversities distributions, according to land use and season (Fig. 2). No differences in mean Bray-Curtis beta pairwise diversities were found in winter season, resulting long-term forest (β_{BC} = 0.58)

conversion to no-till (β_{BC} = 0.57) (Kruskal-Wallis test, χ^2 = 3.6, P_{FDR} = 0.226) or forest conversion to pasture (β_{BC} = 0.57) (χ^2 = 3.6, P_{FDR} = 1), with also no differences between no-till and pasture (χ^2 = 3.6, P_{FDR} = 0.440). Yet for summer, mean pairwise beta diversities decreased after long-term forest (β_{BC} = 0.59) conversion of forest to both no-till (β_{BC} = 0.50) (Kruskal-Wallis test, χ^2 = 232.7, P_{FDR} < 0.001) and pasture (β_{BC} = 0.52) (χ^2 = 232.7, P_{FDR} < 0.001), with diversities in pasture slightly higher than in no-till (χ^2 = 232.7, P_{FDR} = 0.034). When looking for seasonal variation within land uses, we found no differences in beta diversities in forest (χ^2 = 2.5, P_{FDR} = 0.118), with decreases from winter to summer in no-till (χ^2 = 154.2, P_{FDR} < 0.001) and pasture (χ^2 = 55.1, P_{FDR} < 0.001).

Microbial co-occurrence patterns

Overall, network complexity increased after forest conversion to both no-till and pasture and decreased from winter to summer, for both land uses (Fig. 3). Pasture communities presented the highest number of microbial OTUs with at least one significant (P < 0.01) and strong correlation (SparCC > 0.6 or < -0.6), as represented by the number of nodes in both seasons (Table 1). Pasture also showed the highest number of both positive and negative correlations among pairs of OTUs, the highest modularity, the larger network diameter, the larger average path length, and the larger average degree, in both seasons. The number of nodes, the number of edges, the number of positive and negative connections, network diameter, and average path length decreased from winter to summer in all land uses. The number of microbial communities did not vary between seasons for forest but increased in no-till and decreased in pasture, from winter to summer. The average degree decreased from winter to summer for forest and no-till and did not vary for pasture between seasons.

Complementary, we investigated the turnover of microbial abundances across land uses and seasons, according to their habitat specialization, as generalists and specialists (Fig. 4). From a total of 275 OTUs, we found 165 as generalists (60%), 51 specialists in the plateau mesoregion (18.5%), and 59 specialists in the western mesoregion (21.5%). Investigating the seasonal OTUs turnover, in forest (Supplementary Fig. S4a), we found 160 generalists (62%), 48 specialists in winter (19%), and 48 specialists in summer (19%), of which 27 exclusives for forest winter and 11 exclusives for summer. In no-till (Supplementary Fig. S4c), we found 152 generalists (56%), 59 specialists in winter (22%), and 60 specialists in summer (22%), being 25 exclusive for no-till winter and 21 exclusives for summer. In pasture (Supplementary Fig. S4e), we found 139 generalists (54%), 79 specialists in winter (31%), and 40 specialists in summer (15%), of which 36 exclusives for pasture winter and 9 exclusives for summer. We also compared abundance turnover due to land-use change. In long-term forest-to-no-till conversion (Supplementary Fig. S4b), we found 139 generalists (52%), 63 specialists in forest (23%), and 68 specialists in no-till (25%), with 20 exclusive for forest and 14 exclusives for no-till. Yet in long-term forest-to-pasture conversion (Supplementary Fig. S4d), we found 159 generalists (59%), 69 specialists in forest (26%), and 40 specialists in pasture (15%), of which 10 were exclusive for forest and 12 exclusive for pasture. When comparing the differences in assemblages resulting from long-term land-use change (no-till vs. pasture; Supplementary Fig. S4f), we found 149 generalists (55%), 69 specialists in no-till (26%), and 52 specialists in pasture (19%), with 12 exclusives for no-till and 20 exclusives for pasture.

We also sought for potential keystone taxa, the OTUs that hold the networks, as represented by high levels of betweenness centrality—the number of times a node plays a role as a connector between two other nodes, considered an important ecological and

biological feature within a network (Supplementary Table ST2). We found three keystone taxa in forest winter, with no evidence for the presence of keystone OTUs in forest summer. The same as found for no-till, which had three keystone taxa for winter, with no keystone taxa in summer. Yet for pasture, several OTUs seem to be keystone holders in the networks of both winter and summer. When classifying the 20 most important keystone taxa holding each network (Supplementary Table ST2), in terms of habitat specialization, we found: 1) Forest winter: nine out of 20 seasonal specialists and six out of 20 specialists in forest; 2) Forest summer: five out of 20 seasonal specialists and three out of 20 specialists in forest; 3) No-till winter: seven out of 20 seasonal specialists and eight out of 20 specialists in no-till; 4) No-till summer: four out of 20 seasonal specialists and five out of 20 specialists in no-till; 5) Pasture winter: eight out of 20 seasonal specialists and six out of 20 specialists in pasture, and; 6) Pasture summer: three out of 20 seasonal specialists and four out of 20 specialists in pasture.

Distance-decay patterns of beta diversities

To investigate the third significant correlation from PERMANOVA analysis (that is geographic location), we evaluated the DDR patterns of beta pairwise diversities, for bacterial communities and also for generalists and specialists (Fig. 5). Geographical distances between pairs of microbial communities ranged from 0.03 to 397 km. Linear and exponential slopes were significant ($P < 0.001$) for overall bacterial communities (Fig. 5a), generalists (Fig. 5b), and specialists (Fig. 5c), evidencing increases in pairwise Bray-Curtis dissimilarities the extend the distances between pairs of microbial communities increased. We also depicted the variation in distance decay patterns for all land uses and seasons (Supplementary Fig. S5). In winter, we found no differences in linear DDR slopes resulting from long-term conversion of forest (0.046) to no-till (0.048)

533 or pasture (0.046). In summer, the linear slope increased after the long-term conversion
534 of forest (0.045) to pasture (0.055) and decreased after conversion to no-till (0.038).
535 Comparing seasons, linear slopes of forest did not differ. Yet linear slope for no-till
536 decreased from winter (0.048) to summer (0.038) and the opposite was found for pasture,
537 where the slope increased from winter (0.046) to summer (0.055). Exponential slope
538 patterns were similar to those found for linear slopes. In winter, we found no differences
539 resulting from the long-term conversion of forest (8.75E-07) to pasture (8.83E-07), with
540 an increased slope from forest to no-till (9.86E-06). In summer, exponential slopes were
541 similar after long-term conversion of forest (1.09E-06) to pasture (1.05E-06) and
542 decreased after conversion to no-till (8.75E-07). Comparing seasons, the exponential
543 slope of forest increased from winter (8.75E-07) to summer (1.09E-06), the same as for
544 pasture, where the exponential slope varied from 8.83E-07 to 1.05E-06. Yet exponential
545 slope for no-till decreased from winter (9.86E-06) to summer (8.75E-07).
546
547 **Microbial assembly models across land uses and spatial scales**
548 We fitted all the 324 individual samples to theoretical ecological models, according to
549 AIC. From the four tested models, microbial communities fitted predominantly to ZSM
550 neutral model or lognormal niche-based model, with exception of one sample in pasture
551 summer that fitted the preemption niche-based model (Fig. 6a). Most of the samples in
552 forest (61.1%) and no-till (63.9%) fitted the niche-based lognormal distribution, which
553 indicates the prevalence of deterministic processes governing microbial assembly.
554 Otherwise, most of the samples in pasture fitted the ZSM neutral distribution (63.0%),
555 which regards stochastic processes governing assembly. When depicting the seasonal
556 variation in assembly, we found an increase in the number of microbial communities
557 fitting the neutral ZSM assembly from winter to summer, in both forest (35.2 to 42.6%)

and pasture (53.7 to 72.2%). Differently, we observed a decrease in the number of microbial communities fitting the ZSM model from winter (44.5%) to summer (27.8%) in no-till. When comparing the dispersal rates across land uses and seasons (Fig. 6b), through the Kruskal-Wallis test, we observed an increase in the rates of dispersal resulting from the long-term conversion of forest to pasture in both winter (forest, m = 0.082; pasture, m = 0.143; χ^2 = 51.0, $P_{Bonferromi} > 0.001$) and summer ((forest, m = 0.092; pasture, m = 0.147; χ^2 = 51.0, $P_{Bonferromi} > 0.001$), with no differences observed for the forest to no-till conversion, in both seasons, meaning more predisposition to migration from members of pasture local communities, compared with those from forest and no-till. We observed no seasonal effect on dispersal rates for any of the land uses.

When evaluating the influence of geographic distance in assembly patterns, we observed that beta pairwise diversities were lower in local scale—defined as the set of samples within the autocorrelation limit (< 97.196 km; Supplementary Fig. S6)—compared to the regional scale (> 97.196 km) (Figs. 7a and 7b), corroborating the significant DDR observed previously (Fig. 5a). We also found no differences across land uses in winter for both local and regional scales, as observed for overall diversities (See Fig. 2). Diversities decreased in summer on a local scale as a result of the conversion of forest to both no-till and pasture (Fig. 7a), with no significant differences observed at the regional scale, except for no-till, in which beta diversities decreased regionally from winter to summer (Fig. 7b). Comparing diversities within each land use, we found no differences for forest along seasons for local and regional scales. Yet for no-till, diversities decreased in summer in both local and geographic scales. For pasture samples, we noticed that diversities did not differ along seasons in geographic scales, although diversities decreased from winter to summer on a local scale. Thus, we investigated co-occurrence patterns of bacterial OTUs, through Z-scores (Keil, 2019), comparing the

583 observed beta diversities across scales (Figs. 7a and 7b, dark bars), within each land use
584 and season, with the expected diversity resulting from 10000 simulations under the null
585 model (Figs. 7a and 7b, light bars). The resulting Z-score distributions after simulations
586 are presented (Figs. 7c and 7d). At the local scale (Fig. 7c), Z-scores of most forest
587 microbial communities, in winter and summer, fitted the null expectation, the same as for
588 pasture communities, evidencing a neutral assembly, which is expected to occur when
589 selection is weak, and assembly is governed by drift and dispersal processes. Yet for no-
590 till, in both seasons, most of the local communities fitted above the null expectation. Thus,
591 local microbial communities in this environment are more segregated than expected by
592 the null model, which is likely to occur when the variable selection process is acting. At
593 the regional scale (Fig. 7d), Z-scores of forest microbial communities in winter and
594 summer fitted above the null expectation, indicating segregation of communities across
595 geographic distances. A similar trend was found for no-till, where the mean Z-scores were
596 above the null expectation, regarding segregation, but with several communities fitting
597 the null model, neutral. Geographic Z-scores of pasture communities presented the same
598 trends as found for local communities, with most of the communities fitting the null
599 model, in both seasons.
600
601 **Underlying the drivers of microbial community assembly across spatial scales and**
602 **niche occupancies**
603 To evaluate the role of each set of variables (geography + abiotic + biotic) in structuring
604 generalists and specialists decay profiles, we performed Mantel and Partial Mantel tests
605 (Table 2). Mantel tests have shown that the variation in overall bacterial community
606 dissimilarities, considering all land uses together (overall data) was mainly correlated
607 with the biotic factors (Mantel, $\rho = 0.292$, $P = 0.001$), even after controlling for the effect

608 of geographic distance (Partial Mantel, ρ = 0.278, P = 0.001) and abiotic factors (PM, ρ
609 = 0.277, P = 0.001). Significant correlations were also observed with geographic distance
610 (M, ρ = 0.172, P = 0.001) and to a lesser extent with abiotic factors (M, ρ = 0.135, P =
611 0.001). For generalists, the variation was also correlated strongly correlated with the
612 biotic factors (M, ρ = 0.253, P = 0.001), even after controlling for geographic distance
613 (PM, ρ = 0.240, P = 0.001) and abiotic factors (PM, ρ = 0.242, P = 0.001). Significant
614 correlations were also observed with geographic distance (M, ρ = 0.172, P = 0.001), with
615 a minor effect of both geographic distance (M, ρ = 0.157, P = 0.001), and abiotic factors
616 (M, ρ = 0.096, P = 0.001). When looking for the specialists' correlations, the biotic factors
617 (M, ρ = 0.253, P = 0.001) were again the major constraints of dissimilarities distributions,
618 even after controlling for the effect of geographic distance and abiotic factors (M, ρ =
619 0.269, P = 0.001; in both cases). Significant correlations were also observed with abiotic
620 (M, ρ = 0.191, P = 0.001), with a minor effect of geographic distance (M, ρ = 0.160, P =
621 0.001).

622 As we found signals of DDR for both exponential and power-law models (Fig. 5)
623 and also differences in pairwise beta diversities for local and regional scales (Fig. 7), we
624 sought for the evidence of differential patterns of correlations within and over the Moran's
625 I autocorrelation threshold (See supplementary Fig. S6). To achieve that, we divided
626 bacterial, generalists and, specialists dissimilarity matrices according to distance, in local
627 (from 0 to 97.196 km) and regional communities (> 97.196 to 378.160 km). At local scale,
628 the variation in overall bacterial community dissimilarities was mainly correlated with
629 the biotic factors (Table 2) (M, ρ = 0.340, P = 0.001), even after controlling for the effect
630 of geographic distance (Partial Mantel, ρ = 0.299, P = 0.001) and abiotic factors (PM, ρ
631 = 0.309, P = 0.001). Strong and significant correlations were also observed with
632 geographic distance (M, ρ = 0.308, P = 0.001), even controlling for abiotic (PM, ρ =

633 0.297, $P = 0.001$) and biotic factors (PM, $\rho = 0.260$, $P = 0.001$) and to a lesser extent with
634 abiotic factors (M, $\rho = 0.247$, $P = 0.001$), even controlling for geographic distance (PM,
635 $\rho = 0.233$, $P = 0.001$), and biotic factors (PM, $\rho = 0.198$, $P = 0.001$). For generalists, the
636 local variation was also strongly correlated with the biotic factors (M, $\rho = 0.299$, $P =$
637 0.001), even after controlling for geographic distance (PM, $\rho = 0.258$, $P = 0.001$) and
638 abiotic factors (PM, $\rho = 0.277$, $P = 0.001$). Strong and significant correlations were also
639 observed with geographic distance (M, $\rho = 0.285$, $P = 0.001$), even after controlling for
640 biotic distance (PM, $\rho = 0.241$, $P = 0.001$) and abiotic factors distance (PM, $\rho = 0.276$, P
641 $= 0.001$), with a minor effect of abiotic factors (M, $\rho = 0.163$, P = 0.001). Yet for the
642 specialists, we found strong and significant correlations with the three sets of explanatory
643 variables. The biotic factors (M, $\rho = 0.356$, $P = 0.001$) were again the stronger drivers of
644 dissimilarities distributions, even after controlling for the effect of geographic distance
645 and abiotic factors (PM, $\rho = 0.324$, $P = 0.001$; PM, $\rho = 0.318$, $P = 0.001$; respectively).
646 Strong and significant correlations were also observed with abiotic (M, $\rho = 0.325$, $P =$
647 0.001), even controlling for geographic distance and biotic factors (PM, $\rho = 0.315$, $P =$
648 0.001; PM, $\rho = 0.281$, $P = 0.001$; respectively), and to a lesser extent to geographic
649 distance (M, $\rho = 0.243$, $P = 0.001$), even controlling for abiotic and biotic factors (PM, ρ
650 $= 0.229$, $P = 0.001$; PM, $\rho = 0.188$, $P = 0.001$; respectively). Evaluating the mesoregional
651 scale, we observed strong and significant correlations only with biotic factors, for both
652 overall bacterial communities (M, $\rho = 0.231$, $P = 0.001$), generalists (M, $\rho = 0.206$, $P =$
653 0.001), and for specialists (M, $\rho = 0.242$, $P = 0.001$), with lower influence of controlling
654 geographic and abiotic controlling effects.

655 Later, we forward-selected the factors within the sets of significant parameters
656 that could be driving bacterial, generalists, and specialists diversity distributions across
657 spatial scales, through Partial Mantel tests (Table 3). At overall scale, after controlling all

658 the possible individual factors with their respective matrices (e.g. pH controlling for
659 abiotic), the number of nodes was the most important factor for overall bacterial
660 communities (PM, ρ = 0.116, P = 0.002), whereas no strong factor was found for
661 generalists. Yet for specialists, the number of nodes (PM, ρ = 0.205, P = 0.001), and the
662 number of negative edges (PM, ρ = 0.139, P = 0.001), and to a lesser extent spatial
663 distance (PM, ρ = 0.080, P = 0.001), were the main factors. When depicting the variability
664 across spatial scales, we noticed different patterns within and over the mesoregional
665 threshold. At the local scale, spatial distance (PM, ρ = 0.241, P = 0.001), elevation (PM,
666 ρ = 0.227, P = 0.001), and biopores (PM, ρ = 0.140, P = 0.001) were the main drivers of
667 overall bacterial communities. The number of strong and significant correlations was
668 greater for specialists (11 factors) than for generalists (6 factors). Specialists were mainly
669 correlated with spatial distance (PM, ρ = 0.201, P = 0.001), elevation (PM, ρ = 0.155, P
670 = 0.001), season (PM, ρ = 0.133, P = 0.001), number of nodes (PM, ρ = 0.127, P = 0.001),
671 soil type (PM, ρ = 0.108, P = 0.001), and average weighted degree (PM, ρ = 0.106, P =
672 0.001). In comparison, generalists were most correlated with elevation (PM, ρ = 0.228, P
673 = 0.001), spatial distance (PM, ρ = 0.216, P = 0.001), and biopores (PM, ρ = 0.154, P =
674 0.001). At the regional scale, land use (PM, ρ = 0.166, P = 0.001), the number of negative
675 edges (PM, ρ = 0.121, P = 0.001), and the number of nodes (PM, ρ = 0.139, P = 0.001)
676 were the main factors correlated with bacterial communities. Land use (PM, ρ = 0.131, P
677 = 0.001) and negative edges (PM, ρ = 0.122, P = 0.001) were also the major factors for
678 generalists. Yet for specialists the main constraining factors were number of nodes (PM,
679 ρ = 0.240, P = 0.001) and negative edges (PM, ρ = 0.240, P = 0.001), and to a lesser
680 extent land use (PM, ρ = 0.096, P = 0.001).
681
682 **Discussion**

683 The Brazilian Atlantic Forest is recognized as one of the 36 most important hotspots of
684 biodiversity around the globe (Jantz et al. 2015; Weinzettel et al. 2018; de Lima et al.
685 2020), harboring about 1/3 of Brazilian biodiversity and high levels of endemism of both
686 plants and animals (Myers et al. 2000; Ribeiro et al. 2009). As a result, there is an urgent
687 call for the conservation of this threatened and neglected biome. This study has been
688 conceived to advance our understanding of the possible shifts in soil microbial assembly
689 patterns after long-term forest-to-agriculture conversion. Moreover, we have linked the
690 biogeographical patterns of soil microbial communities to the consequences for
691 ecological processes, niche occupancy, and ecosystem services, due to the deforestation
692 of Brazilian tropical and subtropical forests (Mendes et al. 2014, 2015b; Goss-Souza et
693 al. 2019, 2020), focusing on the Subtropical Atlantic Forest (Goss-Souza et al. 2017;
694 Ceola et al. 2021).
695
696 **Drivers of bacterial assembly patterns and processes across spatial scales**
697 Linking microbial diversity patterns to the ecological processes governing assembly has
698 been often implemented for local (Ferrenberg et al. 2013; Dini-Andreote et al. 2014; Jia
699 et al. 2018; Tripathi et al. 2018) or regional and continental scales communities (Stegen
700 et al. 2013; Ma et al. 2016, 2017; Luo et al. 2019), often not taking into account the pure
701 geographic effect of spatial distance (i.e. distance-decays) between microbial
702 communities. Moreover, just a few studies have quantified the coupled effects of spatial
703 distance, abiotic and biotic factors on microbial diversity distribution, and ecological
704 processes (Martiny et al. 2011; Gao et al. 2019; Zhao et al. 2019; Ceola et al. 2021). To
705 our knowledge, this is the first study underlying those patterns and processes for bacterial
706 communities across spatial scales, in Brazilian subtropical soils.

Our first hypothesis claimed that the patterns of microbial assembly would vary along with land uses, and geographic distance between microbial communities, leading to microbial diversity loss due to forest-to-agriculture conversion. Although we did not find differences in alpha diversity and richness (Supplementary Fig. S3), both long-term forest to no-till and forest to pasture conversions led to changes in bacterial beta-diversity distances (Fig. 1) and consequent loss in pairwise beta diversities (Fig. 2), which is indicative of biotic homogenization (Rodrigues et al. 2013; Maaß et al. 2014; Rocha et al. 2021). These results corroborate our previous study, in which we evaluated, through metagenomics, the patterns of microbial alpha and beta diversities in two out of six counties evaluated here (Goss-Souza et al. 2017). Other authors also have found the same soil microbial patterns for both subtropical (Ceola et al. 2021) and tropical soils (Rodrigues et al. 2013; Mendes et al. 2015b). When comparing seasons for the same land use, we found a loss in pairwise beta diversities from winter to summer in no-till and pasture, the same as found in our previous metagenomics study (Goss-Souza et al. 2017). Moreover, our microbial co-occurrence networks have raised the hypothesis that land-use change has not only altered microbial composition and diversity but has also increased the complexity of the biotic interactions among taxa (Fig. 3; Table 1), just as found in other studies (Mendes et al. 2014; Goss-Souza et al. 2017; Felipe-Lucia et al. 2020). Together, our results emphasize that the long-term forest to agriculture conversion led to a loss in microbial diversity, just as observed in previous studies in tropical (Rodrigues et al. 2013; Mendes et al. 2014, 2015b; Goss-Souza et al. 2019, 2020) and subtropical agroecosystems (Goss-Souza et al. 2017; Ceola et al. 2021).

We also found a significant scale-dependence of DDR for overall bacterial communities (Fig. 5; Tables 2 and 3). Fundamentally, this scale dependence was inflated at the local scale (< 97 km) and disappeared at the regional scale, suggesting that,

732 according to Baas Becking proposal, bacterial communities are widespread across the
733 regional limit, and filtered by environmental factors at local scales (De Wit and Bouvier
734 2006). Most microbial studies have highlighted the importance of land-use change and
735 soil physical and chemical characteristics (e.g., pH, soil fertility) as the main drivers of
736 local diversity patterns (Brookes et al. 2010; Rodrigues et al. 2013; Lauber et al. 2013;
737 Mueller et al. 2014). Although we observed a loss in bacterial diversity due to land-use
738 change, markedly in summer (Fig. 2) and a scale dependence for all land uses and seasons
739 (Supplementary Fig. S4), mantel tests revealed that land use was only significant at the
740 regional scale (Table 3), as a secondary effect, explaining 16.6% of the variability. The
741 main drivers at this spatial scale were the biotic factors, as represented the number of
742 nodes (12.1%) and negative edges (15.7%), within other weaker but significant biotic
743 factors, corroborating (Gao et al. 2019). At the local scale, we also found a loss of beta
744 diversities after forest conversion for both no-till and pasture and local scales (Fig. 7a).
745 DDRs were significant for overall bacterial communities across land uses. However, as
746 observed for overall bacterial communities, land use was not a significant factor
747 modulating local microbial diversity, which goes against other findings for local bacterial
748 communities (van der Gast et al. 2011; Hazard et al. 2013; Karimi et al. 2020; Mirza et
749 al. 2020) with season presenting a secondary influence (Table 3). The main drivers of
750 local bacterial communities were spatial distance and elevation. When evaluating the
751 geographical distribution of arbuscular mycorrhizal fungal communities in a broad
752 gradient of land-use intensification and spatial distance, (Ceola et al. 2021) have found
753 significant distance-decays for all land uses, but not directly correlated with the land-use
754 change itself, as the main drivers of decays were soil type, total organic carbon, and clay
755 contents, both considered as evolutionary historical contingencies (Fukami and Nakajima
756 2011), not related to the contemporary human intervention, as represented by land-use

757 change and management intensification. Although we cannot deny that this correlation
758 seems to occur widely, we argue that the arbitrary assignment of soil samples to a
759 determined land use could lead to confounding results. While considering land use as a
760 factor, not a treatment (as we did here), we can observe how this single factor behaves
761 when confronted with other measured or calculated environment characteristics that result
762 from forest to agroecosystem conversion. In this sense, Partial Mantel and Multiple
763 Regression of Matrices (MRM) analyses seem to be powerful tools, as they eliminate the
764 possible collinear effect of a single variable when controlling for the original dataset
765 matrix (Lichstein 2007). Thus, we argue that land uses would not be arbitrarily set as
766 treatments, as soil habitats have multiple facets, due to their geographic location,
767 management intensity, soil type and origin, climate conditions, among others (Fierer and
768 Jackson 2006; Delgado-Baquerizo et al. 2018). Together, those soil ecosystem
769 characteristics culminate with different historical (Fukami and Nakajima 2011) and
770 contemporary contingencies (Durrer et al. 2017; Wang et al. 2017; Karimi et al. 2020),
771 leading to different microbial diversity outcomes (Ceola et al. 2021).

772 In our study, somehow surprisingly, the main filtering factor of bacterial
773 diversities at the overall scale was the number of nodes (biotic factor), explaining 11.6%
774 of the total variation in beta diversities, as revealed by microbial networks and Mantel
775 tests (Table 1; Fig. 3; Table 3). The main local filters were spatial distance and elevation,
776 which together explained 46.8% of the total variation, the same as found in previous
777 biogeographic studies (Fierer and Jackson 2006; Pellissier et al. 2014; Wang et al. 2017;
778 Farrer et al. 2019), with a secondary effect of the season (Goss-Souza et al. 2017; Ma et
779 al. 2017), biopores, an abiotic soil physical factor. The average weighted degree was the
780 major biotic filter of bacterial communities at the local scale (11.9%), corroborating the
781 findings of a biogeographic study of bacterial communities in paddy soils at a continental

782 scale (Gao et al. 2019). The authors also found coupled effect of geographic distance,
783 abiotic and biotic factors, as observed in our study. Those observations are in contrast
784 with several studies that have attributed this local filtering predominantly to habitat
785 characteristics that lead to environmental abiotic selection (Julia et al. 2014; Mendes et
786 al. 2015a; Durrer et al. 2017).

787 Another possible explanation for the significant DDRs is dispersal limitation, as
788 observed by the low immigration rates we have calculated in our study, particularly for
789 forest and no-till microbial communities (Fig. 6b). These findings are following what we
790 have observed in a metagenomic study where we compared the same land uses in two out
791 of the six counties of the present study (Goss-Souza et al. 2017). Some shreds of evidence
792 against the Baas Becking hypothesis come from studies showing that dispersal of
793 microbes is limited, meaning that "everything is not everywhere", at least at a
794 contemporary pace (Nemergut et al. 2013). By comparing the DDRs of bacterial
795 communities with the patterns found for Eukaryotes, including Fungi (Zhao et al. 2019;
796 Ceola et al. 2021), the decays tend to be lower for Bacteria, but they are often significant,
797 meaning that the higher the distance between pairs of microbial communities, the more
798 contrasting they are (Horner-Devine et al. 2004; Martiny et al. 2006, 2011; Gao et al.
799 2019). All those results together led us to partially reject our first hypothesis, since the
800 land-use change, despite being significant, was not found as a ruling driver of microbial
801 assembly patterns.

802 Our second hypothesis stated that (ii) the balance between neutral and niche-based
803 assembly models would differ along land uses, and spatial scales. Our theoretical rank
804 association models based on AIC (Fig. 6a) showed that forest and no-till soil samples
805 fitted most a niche-based model (Lognormal), regarding deterministic assembly processes
806 while pasture soil samples fitted most a neutral-based model (ZSM), related to stochastic

807 assembly processes. Moreover, we observed that the balance between stochastic and
808 deterministic assembly varied from winter to summer season, partially confirming our
809 second hypothesis. Once more, our T-RFLP data corroborated our previous
810 metagenomics data (Goss-Souza et al. 2017), suggesting that forest and no-till microbial
811 communities have a niche-based assembly, related to deterministic processes, suggesting
812 that they are more likely to be governed by environmental filtering through the ecological
813 selection process (Stegen et al. 2013; Dini-Andreote et al. 2015). Conversely, pasture
814 communities have a predominantly neutral assembly, regarding stochastic processes
815 modulating microbial assembly patterns, indicating a pivotal role of dispersal ecological
816 process (Albright et al. 2019; Li et al. 2020). We also found a positive correlation between
817 dispersal rates and microbial communities fitting neutral assembly, with pasture samples
818 presenting both higher values of dispersal rates and more samples fitting to stochastic
819 ZSM rank abundance model (Fig. 6b). Together, these results confirm previous
820 theoretical and experimental models suggesting that dispersal has an important role in
821 structuring microbial communities assembly (Hubbell 2005; Martiny et al. 2011;
822 Ferrenberg et al. 2013; Nemergut et al. 2013; Goss-Souza et al. 2020).

823 Therefore, we depicted the balance between neutral- and niche-based assembly
824 models, according to spatial distance, through Z-scores. At the local scale, we found that
825 forest microbial communities presented, on average, a neutral-based model, related to
826 stochastic processes, but with a large interplay between neutral and niche-based
827 assembly, mainly in the winter season (as represented by the high standard deviation;
828 boxplot, Fig. 7c). No-till microbial communities fitted above the neutral threshold of
829 deviation from null expectation (+2), which indicated that communities were more
830 segregated than expected by chance, regarding deterministic variable selection (Dini-
831 Andreote et al. 2015; Gao et al. 2019; Xue et al. 2021). Yet for pasture, most communities

fitted within the neutral-based assembly, regarding stochastic processes, the same as found in our previous metagenomics study (Goss-Souza et al. 2017). At the regional scale (Fig. 7d), forest microbial communities followed a niche-based model, related to deterministic variable selection, differently from what we have found at overall and local scales, but corroborating (Goss-Souza et al. 2017). No-till communities fitted above the null expectation, regarding variable selection, the same as found at the local scale. Meanwhile, pasture communities fitted within the neutral-based assembly, regarding stochastic processes, the same as found for overall and local scales. Ecologically, the assembly of microbial communities is dependent on the trade-offs between local and regional microbial communities, which is dependent on the microbial survival at the local species pool and the colonization potential of microbial species in the regional pool (Pärtel et al. 2017; Bittleston et al. 2020). While distance-decays and dispersal acted on the composition of microbial communities, variable selection and drift altered the relative abundances. Our findings have demonstrated an interplay among stochastic and deterministic processes modulating assembly, at temporal and spatial scales, the same as found for other soil and synthetic microbial communities (Ferrenberg et al. 2013; Nemergut et al. 2013; Stegen et al. 2013; Dini-Andreote et al. 2015; Evans et al. 2017; Goss-Souza et al. 2017, 2020; König et al. 2019).

Biogeographic patterns and assembly processes differ between generalists and specialists

Ecologists have long-established the conceptual basis of niche occupancy and habitat specialization for several species of plants and animals (Reznick et al. 2002; Bohn et al. 2014). Several authors have raised the idea of examining microbial life-history strategies to comprehend the patterns and processes that modulate species distribution and trophic

857 relationships in soils (van der Heyde et al. 2017; Powell and Rillig 2018). Here, we
858 separated species as generalists and specialists, based on the frequency of occurrence and
859 habitat specialization of each OTU into our 324 samples representing bacterial
860 communities. Our third hypothesis affirmed that (iii) the processes governing microbial
861 assembly would vary between habitat generalists and specialists. Our results have shown
862 that forest microbial communities presented the highest proportion of specialists but the
863 lowest values of betweenness centrality, while pasture has presented an opposite pattern.
864 The betweenness centrality is defined as the number of times a node (i.e. taxa) acts as a
865 bridge along the shortest path between two other nodes, which indicates the most
866 important nodes that are interpreted as key taxa with a central role in the community
867 (Poudel et al. 2016; Mendes et al. 2018; Shi et al. 2020). This result indicates that forest
868 communities have presented a higher number of keystones species that are responsible
869 for regulating the structure and dynamics of the community network. On the other hand,
870 pasturelands have presented few keystone taxa but with a higher betweenness centrality.
871 Key taxa are associated with many others, and the removal of these nodes may have a
872 large impact on the community structure (Steele et al. 2011). Thus, the lower number of
873 specialists and keystone species in pasture suggest a less resilient and stress-tolerant
874 community.

875 As land use did not play a pivotal role in separating bacterial species diversity and
876 distributions, we depicted the overall bacterial OTU patterns and the spatial scale effect,
877 according to microbial life strategies (Barberán et al. 2012; Leff et al. 2015; Gao et al.
878 2019; Luo et al. 2019). The most prevalent OTUs in our study were found as habitat
879 specialists. Our CLAM tests (Fig. 4) coupled with DDRs (Fig. 5) strongly support a
880 perspective of microbial distribution in which communities are dominated by endemic
881 species and share very few common OTUs between sites and along geographical

882 gradients (Robeson et al. 2011). This local endemism thesis is here supported by the great
883 influence of dispersal limitation in overall assembly patterns (Figs. 5, 6, and 7). Moreover,
884 the endemic distribution is emphasized by the high significance of geographical distance
885 at the local scale for overall communities (Tables 2 and 3), coupled with the interaction
886 with biotic factors at the local scale for endemic OTUs, just as found in another
887 biogeographic study (Gao et al. 2019). Our DDRs for endemic taxa have shown that
888 decays culminated with high pairwise diversities at larger distances (Luo et al. 2019),
889 directly contradicting the idea of "everything is everywhere". It suggests that the diversity
890 of soil microbial communities, such as the ones found in the Atlantic Forest biome in our
891 study, might be "beyond the borders" of our previous speculations, especially given the
892 prevalence of endemic microbial species. Linking these endemic patterns found for
893 microbial communities in our study with the already existent knowledge about high levels
894 of endemism of animals and, especially plants in the Atlantic forest biome and other
895 global hotspots of biodiversity (Myers et al. 2000; Jantz et al. 2015) is paramount. It also
896 raises the hypothesis that, land use, as a contemporary paced human intervention, it is not
897 a pivotal shaper of microbial niche occupancy and habitat specialization. As we have
898 found in a previous study of AM fungal biogeography in this same biome (Ceola et al.
899 2021), land use was only significant for overall bacterial communities and generalists and
900 at a regional scale. Our results have shown that other historical contingencies (Fukami
901 and Nakajima 2011; Ceola et al. 2021), as represented by soil type, and seasonal effect,
902 intimately linked to soil formation (Tables 2 and 3), and evolutionary contingencies
903 (Hanson et al. 2012; Wang et al. 2013), linked to dispersal limitation (Figs. 6 and 7) and
904 taxa evolution, may be driving microbial niche breadth (Luo et al. 2019) and habitat
905 specialization (Székely and Langenheder 2014), markedly at local scales. Also, those
906 historical and evolutionary contingencies could be shaping microbial co-occurrence

907 patterns and interacting with biotic deterministic selection (i.e. variable selection)
908 (Barberán et al. 2012; Dini-Andreote et al. 2015; Gao et al. 2019).

909 Soil type is defined by geological and climatic historical contingencies, which
910 together with the activity of microorganisms, water and time regulate rock intemperism
911 and soil formation (Huggett 1998; Egli et al. 2018). According to the World Reference
912 Base for Soil Resources (Anjos et al. 2015), the soils from all sampling sites in the western
913 mesoregion are classified as Red Ferralsols, which are evolved soils with the dominance
914 of kaolinite and Fe oxides. Otherwise, soils from plateau mesoregion are more diverse.
915 Soils from the counties of Lages and Campo Belo do Sul, were classified as Humic
916 Yellow Nitisols, which are strongly structured soils, characterized by low-activity clay, P
917 fixation, the prevalence of Fe oxides, and accumulation of organic matter in the surface
918 while soils from Otacílio Costa County were found to be Humic Cambisols, which are
919 soils with little or no profile differentiation, moderately developed, with the accumulation
920 of organic matter in the surface. We argue that soil type, a historical contingency (together
921 with dispersal, an evolutionary contingency), could be locally filtering taxa distributions
922 more strongly than the influence of land-use change, which is historically recent, as all
923 the sites were converted from the forest into agroecosystems in the last decades (Bartz et
924 al. 2014; Goss-Souza et al. 2017; Ceola et al. 2021).

925 We can reach a more comprehensive view of biodiversity, by integrating
926 belowground microbial diversity and aboveground plant diversity, when studying
927 microbial communities in terms of shifts in relative abundances using weighted
928 resemblances (e.g. Bray-Curtis), as we performed here. Some theoretical reviews and
929 experimental studies have shown that applying those simpler rules and resolutions would
930 allow ecologists to integrate microbial and macrobial patterns of diversity (Soininen et al.
931 2007; Astorga et al. 2012; Shade et al. 2018). In our case, these implementations will

allow, in the next step, comparisons between belowground microbial diversity and aboveground plant diversity patterns, to advance our understanding of how the historical contingencies could be driving not only macrobial endemism (Myers et al. 2000; Vale et al. 2018) in the Atlantic Forest biome but also the microbial endemism, as observed in the present and previous studies from our group (Goss-Souza et al. 2017; Ceola et al. 2021). As an outcome, those linked results will enable ecologists to gather important datasets for land occupation, use, and management modeling. Meanwhile, policymakers may use this integrative information for establishing environmental monitoring and conservation strategies, to safeguard supporting ecosystem services, dependent on microbial activity (e.g. carbon and nutrient cycling), which are linked to provisioning and regulating services, such as food production, carbon storage, and GHG emissions/mitigation at the Atlantic Forest and other subtropical and tropical hotspots of biodiversity.

Conclusions

This study represented a step forward to depict the biogeographic patterns of bacterial communities due to land-use change in a broader geographic scale, in the subtropical Atlantic Forest biome. We have shown that soil bacterial diversity and niche occupancy are shaped by geographic spatial distance and long-term historical contingencies related to the soil origin (e.g. soil type and climate), that culminate with important coupled patterns of dispersal limitation and significant distance-decays of beta diversities. We also demonstrated that—differently from the "everything is everywhere" niche postulation—stochastic processes, represented by the dispersal limitation act to outweigh the effect of the deterministic selection process caused by soil historical contingencies and the formation of small geographic islands, shaped by soil type and climate. Those patterns

957 are inflated when evaluation microbial niche specialists, markedly at a local scale, with
958 consequences for biotic interactions among members from local microbial communities.
959 Differently from several other microbiological local and biogeographical studies, land-
960 use change was not found a major driver of microbial patterns and processes.

961

962 **References**

963 Albright MBN, Chase AB, Martiny JBH (2019) Experimental Evidence that
964 Stochasticity Contributes to Bacterial Composition and Functioning in a
965 Decomposer Community. MBio 10:1–13. https://doi.org/10.1128/mbio.00568-19
966 Alef K, Nannipieri P (1995) Methods in Applied Soil Microbiology and Biochemistry,
967 1st edn. Elsevier, London
968 Anderson MJ (2001) A new method for non-parametric multivariate analysis of
969 variance. Austral Ecol 26:32–46. https://doi.org/10.1046/j.1442-
970 9993.2001.01070.x
971 Anderson TH, Domsch KH (1993) The metabolic quotient for CO2 (qCO2) as a
972 specific activity parameter to assess the effects of environmental conditions, such
973 as pH, on the microbial biomass of forest soils. Soil Biol Biochem 25:393–395.
974 https://doi.org/10.1016/0038-0717(93)90140-7
975 Anjos L, Gaistardo, Carlos Cruz; Deckers J, Dondeyne, Stefaan; Eberhardt, Einar;
976 Gerasimova M, et al (2015) World reference base for soil resources 2014
977 International soil classification system for naming soils and creating legends for
978 soil maps. FAO, Rome
979 Astorga A, Oksanen J, Luoto M, et al (2012) Distance decay of similarity in freshwater
980 communities: Do macro- and microorganisms follow the same rules? Glob Ecol
981 Biogeogr 21:365–375. https://doi.org/10.1111/j.1466-8238.2011.00681.x
982 Barberán A, Bates ST, Casamayor EO, Fierer N (2012) Using network analysis to
983 explore co-occurrence patterns in soil microbial communities. ISME J 6:343–351.
984 https://doi.org/10.1038/ismej.2011.119
985 Bartz MLC, Brown GG, da Rosa MG, et al (2014) Earthworm richness in land-use
986 systems in Santa Catarina, Brazil. Appl Soil Ecol 83:59–70.
987 https://doi.org/10.1016/j.apsoil.2014.03.003
988 Baselga A (2017) Partitioning abundance-based multiple-site dissimilarity into

components: balanced variation in abundance and abundance gradients. Methods Ecol Evol 8:799–808. https://doi.org/10.1111/2041-210X.12693

Baselga A, Orme D, Villeger S, et al (2018) betapart: Partitioning Beta Diversity into Turnover and Nestedness Components.

Bastian M, Heymann S, Jacomy M (2009) Gephi: an open source software for exploring and manipulating networks. In: International AAAI Conference on Weblogs and Social Media. San Jose

Bittleston LS, Gralka M, Leventhal GE, et al (2020) Context-dependent dynamics lead to the assembly of functionally distinct microbial communities. Nat Commun 11:1–10. https://doi.org/10.1038/s41467-020-15169-0

Blanchet FG, Cazelles K, Gravel D (2020) Co-occurrence is not evidence of ecological interactions. Ecol Lett 23:1050–1063

Bohn K, Pavlick R, Reu B, Kleidon A (2014) The strengths of r- And K-selection shape diversity-disturbance relationships. PLoS One 9:e95659. https://doi.org/10.1371/journal.pone.0095659

Bozdogan H (1987) Model selection and Akaike's Information Criterion (AIC): The general theory and its analytical extensions. Psychometrika 52:345–370. https://doi.org/10.1007/BF02294361

Brinkmann N, Schneider D, Sahner J, et al (2019) Intensive tropical land use massively shifts soil fungal communities. Sci Rep 9:1–11. https://doi.org/10.1038/s41598-019-39829-4

Brody JR, Kern SE (2004) Sodium boric acid: a Tris-free, cooler conductive medium for DNA electrophoresis. Biotechniques 36:214–216

Brookes PC, Lauber CL, Rousk J, et al (2010) Soil bacterial and fungal communities across a pH gradient in an arable soil. 1340–1351. https://doi.org/10.1038/ismej.2010.58

Cambardella CA, Elliott ET (1992) Particulate Soil Organic-Matter Changes across a Grassland Cultivation Sequence. Soil Sci Soc Am J 56:777–783. https://doi.org/10.2136/sssaj1992.03615995005600030017x

Ceola G, Goss-Souza D, Alves J, et al (2021) Biogeographic Patterns of Arbuscular Mycorrhizal Fungal Communities Along a Land-Use Intensification Gradient in the Subtropical Atlantic Forest Biome. Microb Ecol. https://doi.org/10.1007/s00248-021-01721-y

Chazdon RL, Chao A, Colwell RK, et al (2011) A novel statistical method for

1023 classifying habitat generalists and specialists. Ecology 92:1332–1343.
1024 https://doi.org/10.1890/10-1345.1
1025 Claessen MEC, Barreto WO, Paula JL, Duarte MN (1997) Manual of soil analysis
1026 methods, 2nd edn. Embrapa, Rio de Janeiro
1027 Cordovez V, Dini-Andreote F, Carrión VJ, Raaijmakers JM (2019) Ecology and
1028 Evolution of Plant Microbiomes. Annu Rev Microbiol 73:annurev-micro-090817-
1029 062524. https://doi.org/10.1146/annurev-micro-090817-062524
1030 Cottenie K (2005) Integrating environmental and spatial processes in ecological
1031 community dynamics. Ecol Lett 8:1175–1182. https://doi.org/10.1111/j.1461-
1032 0248.2005.00820.x
1033 Creamer RE, Hannula SE, Leeuwen JPV, et al (2016) Ecological network analysis
1034 reveals the inter-connection between soil biodiversity and ecosystem function as
1035 affected by land use across Europe. Appl Soil Ecol 97:112–124.
1036 https://doi.org/10.1016/j.apsoil.2015.08.006
1037 de Lima RAF, Oliveira AA, Pitta GR, et al (2020) The erosion of biodiversity and
1038 biomass in the Atlantic Forest biodiversity hotspot. Nat Commun 11:1–16.
1039 https://doi.org/10.1038/s41467-020-20217-w
1040 De Vrieze J, Ijaz UZ, Saunders AM, Theuerl S (2018) Terminal restriction fragment
1041 length polymorphism is an “old school” reliable technique for swift microbial
1042 community screening in anaerobic digestion. Sci Rep 8:20–22.
1043 https://doi.org/10.1038/s41598-018-34921-7
1044 De Wit R, Bouvier T (2006) “Everything is everywhere, but, the environment selects”;
1045 what did Baas Becking and Beijerinck really say? Environ Microbiol 8:755–758.
1046 https://doi.org/10.1111/j.1462-2920.2006.01017.x
1047 Delgado-Baquerizo M, Oliverio AM, Brewer TE, et al (2018) A global atlas of the
1048 dominant bacteria found in soil. Science (80-) 359:320–325.
1049 https://doi.org/10.1126/science.aap9516
1050 Dexter AR (1988) Advances in characterization of soil structure. Soil Tillage Res
1051 11:199–238
1052 Dexter AR, Czyz EA, Gaţe OP (2007) A method for prediction of soil penetration
1053 resistance. Soil Tillage Res 93:412–419. https://doi.org/10.1016/j.still.2006.05.011
1054 Dhaliwal GS, Gupta N, Kukal SS, Kaur M (2011) Standardization of automated Vario
1055 EL III CHNS analyzer for total carbon and nitrogen determination in soils.
1056 Commun Soil Sci Plant Anal 42:971–979.

https://doi.org/10.1080/00103624.2011.558965

Dini-Andreote F, de Cássia Pereira e Silva M, Triadó-Margarit X, et al (2014) Dynamics of bacterial community succession in a salt marsh chronosequence: evidences for temporal niche partitioning. ISME J 8:1989–2001. https://doi.org/10.1038/ismej.2014.54

Dini-Andreote F, Stegen JC, van Elsas JD, Salles JF (2015) Disentangling mechanisms that mediate the balance between stochastic and deterministic processes in microbial succession. Proc Natl Acad Sci 201414261. https://doi.org/10.1073/pnas.1414261112

Dumbrell AJ, Nelson M, Helgason T, et al (2010) Relative roles of niche and neutral processes in structuring a soil microbial community. ISME J 4:337–345. https://doi.org/10.1038/ismej.2009.122

Durrer A, Gumiere T, Taketani RG, et al (2017) The drivers underlying biogeographical patterns of bacterial communities in soils under sugarcane cultivation. Appl Soil Ecol 110:12–20. https://doi.org/10.1016/j.apsoil.2016.11.005

Edwards U, Rogall T, Blöcker H, et al (1989) Isolation and direct complete nucleotide determination of entire genes. Characterization of a gene coding for 16S ribosomal RNA. Nucleic Acids Res 17:7843–7853. https://doi.org/10.1093/nar/17.19.7843

Egli M, Hunt AG, Dahms D, et al (2018) Prediction of soil formation as a function of age using the percolation theory approach. Front Environ Sci 6:1–21. https://doi.org/10.3389/fenvs.2018.00108

Etienne RS, Alonso D (2005) A dispersal-limited sampling theory for species and alleles. Ecol Lett 8:1147–1156. https://doi.org/10.1111/j.1461-0248.2005.00817.x

Evans S, Martiny JBH, Allison SD (2017) Effects of dispersal and selection on stochastic assembly in microbial communities. ISME J 11:176–185. https://doi.org/10.1038/ismej.2016.96

Fan K, Cardona C, Li Y, et al (2017) Rhizosphere-associated bacterial network structure and spatial distribution differ significantly from bulk soil in wheat crop fields. Soil Biol Biochem 113:275–284. https://doi.org/10.1016/j.soilbio.2017.06.020

Faoro H, Alves AC, Souza EM, et al (2010) Influence of soil characteristics on the diversity of bacteria in the southern brazilian atlantic forest. Appl Environ Microbiol 76:4744–4749. https://doi.org/10.1128/AEM.03025-09

Farrer EC, Porazinska DL, Spasojevic MJ, et al (2019) Soil Microbial Networks Shift Across a High-Elevation Successional Gradient. Front Microbiol 10:1–13.

https://doi.org/10.3389/fmicb.2019.02887

Felipe-Lucia MR, Soliveres S, Penone C, et al (2020) Land-use intensity alters networks between biodiversity, ecosystem functions, and services. Proc Natl Acad Sci 117:28140–28149. https://doi.org/10.1073/pnas.2016210117

Feng M, Tripathi BM, Shi Y, et al (2019) Interpreting distance- decay pattern of soil bacteria via quantifying the assembly processes at multiple spatial scales. Microbiologyopen e851. https://doi.org/10.1002/mbo3.851

Ferrenberg S, O'Neill SP, Knelman JE, et al (2013) Changes in assembly processes in soil bacterial communities following a wildfire disturbance. ISME J 7:1102–1111. https://doi.org/10.1038/ismej.2013.11

Fierer N, Jackson RB (2006) The diversity and biogeography of soil bacterial communities. Proc Natl Acad Sci U S A 103:626–631. https://doi.org/10.1073/pnas.0507535103

Friedman J, Alm EJ (2012) Inferring Correlation Networks from Genomic Survey Data. PLoS Comput Biol 8:1–11. https://doi.org/10.1371/journal.pcbi.1002687

Fukami T, Nakajima M (2011) Community assembly: Alternative stable states or alternative transient states? Ecol Lett 14:973–984. https://doi.org/10.1111/j.1461-0248.2011.01663.x

Gao Q, Yang Y, Feng J, et al (2019) The spatial scale dependence of diazotrophic and bacterial community assembly in paddy soil. Glob Ecol Biogeogr 28:1093–1105. https://doi.org/10.1111/geb.12917

Gee GW, Bauder JW (1986) Particle-size analysis. In: Klute A (ed) Methods of soil analysis. ASA, Madison, pp 383–411

Gómez-Rodríguez C, Baselga A (2018) Variation among European beetle taxa in patterns of distance decay of similarity suggests a major role of dispersal processes. Ecography (Cop) 41:1825–1834. https://doi.org/10.1111/ecog.03693

Goss-Souza D, Mendes LW, Borges CD, et al (2017) Soil microbial community dynamics and assembly under long-term land use change. FEMS Microbiol Ecol 93:fix109. https://doi.org/10.1093/femsec/fix109

Goss-Souza D, Mendes LW, Rodrigues JLM, Tsai SM (2019) Amazon forest-to-agriculture conversion alters rhizosphere microbiome composition while functions are kept. FEMS Microbiol Ecol 95:fiz009. https://doi.org/10.1093/femsec/fiz009

Goss-Souza D, Mendes LW, Rodrigues JLM, Tsai SM (2020) Ecological Processes Shaping Bulk Soil and Rhizosphere Microbiome Assembly in a Long-Term

1125 Amazon Forest-to-Agriculture Conversion. Microb Ecol 79:110–122.
1126 https://doi.org/10.1007/s00248-019-01401-y
1127 Hanson CA, Fuhrman JA, Horner-Devine MC, Martiny JBH (2012) Beyond
1128 biogeographic patterns: Processes shaping the microbial landscape. Nat Rev
1129 Microbiol 10:497–506. https://doi.org/10.1038/nrmicro2795
1130 Hazard C, Gosling P, Van Der Gast CJ, et al (2013) The role of local environment and
1131 geographical distance in determining community composition of arbuscular
1132 mycorrhizal fungi at the landscape scale. ISME J 7:498–508.
1133 https://doi.org/10.1038/ismej.2012.127
1134 Horner-Devine MC, Lage M, Hughes JB, Bohannan BJM (2004) A taxa-area
1135 relationship for bacteria. Nature 432:750–753. https://doi.org/10.1038/nature03073
1136 Hovatter SR, Dejelo C, Case AL, Blackwood CB (2011) Metacommunity organization
1137 of soil microorganisms depends on habitat defined by presence of Lobelia
1138 siphilitica plants. Ecology 92:57–65
1139 Hubbell SP (2005) Neutral theory in community ecology and the hypothesis of
1140 functional equivalence. Funct Ecol 19:166–172. https://doi.org/10.1111/j.0269-
1141 8463.2005.00965.x
1142 Huggett RJ (1998) Soil chronosequences, soil development, and soil evolution: A
1143 critical review. Catena 32:155–172. https://doi.org/10.1016/S0341-8162(98)00053-
1144 8
1145 Jabot F, Etienne RS, Chave J (2008) Reconciling neutral community models and
1146 environmental filtering: Theory and an empirical test. Oikos.
1147 https://doi.org/10.1111/j.0030-1299.2008.16724.x
1148 Jantz SM, Barker B, Brooks TM, et al (2015) Future habitat loss and extinctions driven
1149 by land-use change in biodiversity hotspots under four scenarios of climate-change
1150 mitigation. Conserv Biol 29:1122–1131. https://doi.org/10.1111/cobi.12549
1151 Jesus EC, Marsh TL, Tiedje JM, Moreira FM (2009) Changes in land use alter the
1152 structure of bacterial communities in Western Amazon soils. ISME J 3:1004–1011.
1153 https://doi.org/10.1038/ismej.2009.47
1154 Jia X, Dini-Andreote F, Falcão Salles J (2018) Community Assembly Processes of the
1155 Microbial Rare Biosphere. Trends Microbiol.
1156 https://doi.org/10.1016/j.tim.2018.02.011
1157 Jones CM, Hallin S (2019) Geospatial variation in co-occurrence networks of nitrifying
1158 microbial guilds. Mol Ecol 28:293–306. https://doi.org/10.1111/mec.14893

1159 Julia M, Brossi DL, Mendes LW, et al (2014) Assessment of Bacterial bph Gene in
1160 Amazonian Dark Earth and Their Adjacent Soils. 9:.
1161 https://doi.org/10.1371/journal.pone.0099597
1162 Kaiser K, Wemheuer B, Korolkow V, et al (2016) Driving forces of soil bacterial
1163 community structure, diversity, and function in temperate grasslands and forests.
1164 Sci Rep 6:1–12. https://doi.org/10.1038/srep33696
1165 Karczewski K, Riss HW, Meyer EI (2017) Comparison of DNA-fingerprinting (T-
1166 RFLP) and high-throughput sequencing (HTS) to assess the diversity and
1167 composition of microbial communities in groundwater ecosystems. Limnologica
1168 67:45–53. https://doi.org/10.1016/j.limno.2017.10.001
1169 Kari A, Nagymáté Z, Romsics C, et al (2019) Monitoring of soil microbial inoculants
1170 and their impact on maize (Zea mays L.) rhizosphere using T-RFLP molecular
1171 fingerprint method. Appl Soil Ecol 138:233–244.
1172 https://doi.org/10.1016/j.apsoil.2019.03.010
1173 Karimi B, Villerd J, Dequiedt S, et al (2020) Biogeography of soil microbial habitats
1174 across France. Glob Ecol Biogeogr 29:1399–1411.
1175 https://doi.org/10.1111/geb.13118
1176 Keeney DR, Nelson DW (1982) Nitrogen - inorganic forms. In: Page AL (ed) Methods
1177 in Soil Analysis, part 2, 2nd edn. ASA and SSSA, Madison, pp 643–698
1178 Keil P (2019) Z-scores unite pairwise indices of ecological similarity and association
1179 for binary data. Ecosphere 10:1–7. https://doi.org/10.1002/ecs2.2933
1180 König S, Köhnke MC, Firle A-L, et al (2019) Disturbance Size Can Be Compensated
1181 for by Spatial Fragmentation in Soil Microbial Ecosystems. Front Ecol Evol 7:1–
1182 11. https://doi.org/10.3389/fevo.2019.00290
1183 Lange M, Eisenhauer N, Sierra CA, et al (2015) Plant diversity increases soil microbial
1184 activity and soil carbon storage. Nat Commun 6:.
1185 https://doi.org/10.1038/ncomms7707
1186 Lauber CL, Ramirez KS, Aanderud Z, et al (2013) Temporal variability in soil
1187 microbial communities across land-use types. ISME J 7:1641–1650.
1188 https://doi.org/10.1038/ismej.2013.50
1189 Leff JW, Jones SE, Prober SM, et al (2015) Consistent responses of soil microbial
1190 communities to elevated nutrient inputs in grasslands across the globe. Proc Natl
1191 Acad Sci U S A 112:10967–10972. https://doi.org/10.1073/pnas.1508382112
1192 Legendre P, Fortin M-J (1989) Spatial pattern and ecological analysis. Vegetatio

80:107–138

Leibold MA, Holyoak M, Mouquet N, et al (2004) The metacommunity concept: a framework for multi-scale community ecology. Ecol Lett 7:601–613. https://doi.org/10.1111/j.1461-0248.2004.00608.x

Lepš J, Šmilauer P (2005) Multivariate Analysis of Ecological Data using CANOCO. Bull Ecol Soc Am 86:6–6. https://doi.org/10.1890/0012-9623(2005)86[6a:MAOEDU]2.0.CO;2

Li S peng, Wang P, Chen Y, et al (2020) Island biogeography of soil bacteria and fungi: similar patterns, but different mechanisms. ISME J 14:1886–1896. https://doi.org/10.1038/s41396-020-0657-8

Li X, Jousset A, de Boer W, et al (2019) Legacy of land use history determines reprogramming of plant physiology by soil microbiome. ISME J 13:738–751. https://doi.org/10.1038/s41396-018-0300-0

Li Y, Wu X, Chen T, et al (2018) Plant phenotypic traits eventually shape its microbiota: A common garden test. Front Microbiol 9:1–13. https://doi.org/10.3389/fmicb.2018.02479

Lichstein JW (2007) Multiple regression on distance matrices: A multivariate spatial analysis tool. Plant Ecol 188:117–131. https://doi.org/10.1007/s11258-006-9126-3

Luo Z, Liu J, Zhao P, et al (2019) Biogeographic patterns and assembly mechanisms of bacterial communities differ between habitat generalists and specialists across elevational gradients. Front Microbiol 10:1–14. https://doi.org/10.3389/fmicb.2019.00169

Ma B, Dai Z, Wang H, et al (2017) Distinct Biogeographic Patterns for Archaea, Bacteria, and Fungi along the Vegetation Gradient at the Continental Scale in Eastern China. mSystems 2:1–14. https://doi.org/10.1128/msystems.00174-16

Ma B, Wang H, Dsouza M, et al (2016) Geographic patterns of co-occurrence network topological features for soil microbiota at continental scale in eastern China. ISME J 10:1891–1901. https://doi.org/10.1038/ismej.2015.261

Maaß S, Migliorini M, Rillig MC, Caruso T (2014) Disturbance, neutral theory, and patterns of beta diversity in soil communities. Ecol Evol 4:4766–4774. https://doi.org/10.1002/ece3.1313

Martiny JBH, Bohannan BJM, Brown JH, et al (2006) Microbial biogeography: Putting microorganisms on the map. Nat Rev Microbiol 4:102–112. https://doi.org/10.1038/nrmicro1341

1227 Martiny JBH, Eisen JA, Penn K, et al (2011) Drivers of bacterial β-diversity depend on
1228 spatial scale. Proc Natl Acad Sci U S A 108:7850–7854.
1229 https://doi.org/10.1073/pnas.1016308108
1230 Mendes LW, de Lima Brossi MJ, Kuramae EE, Tsai SM (2015a) Land-use system
1231 shapes soil bacterial communities in Southeastern Amazon region. Appl Soil Ecol
1232 95:151–160. https://doi.org/10.1016/j.apsoil.2015.06.005
1233 Mendes LW, Kuramae EE, Navarrete AA, et al (2014) Taxonomical and functional
1234 microbial community selection in soybean rhizosphere. ISME J 8:1–11.
1235 https://doi.org/10.1038/ismej.2014.17
1236 Mendes LW, Raaijmakers JM, De Hollander M, et al (2018) Influence of resistance
1237 breeding in common bean on rhizosphere microbiome composition and function.
1238 ISME J 12:212–224. https://doi.org/10.1038/ismej.2017.158
1239 Mendes LW, Tsai SM, Navarrete AA, et al (2015b) Soil-Borne Microbiome: Linking
1240 Diversity to Function. Microb Ecol 70:255–265. https://doi.org/10.1007/s00248-
1241 014-0559-2
1242 Meyer KM, Klein AM, Rodrigues JLM, et al (2017) Conversion of Amazon rainforest
1243 to agriculture alters community traits of methane-cycling organisms. Mol Ecol
1244 26:1547–1556. https://doi.org/10.1111/mec.14011
1245 Meyer KM, Memiaghe H, Korte L, et al (2018) Why do microbes exhibit weak
1246 biogeographic patterns? ISME J 12:1404–1413. https://doi.org/10.1038/s41396-
1247 018-0103-3
1248 Mirza BS, McGlinn DJ, Bohannan BJM, et al (2020) Diazotrophs show signs of
1249 restoration in Amazon rain forest soils with ecosystem rehabilitation. Appl Environ
1250 Microbiol 86:1–10. https://doi.org/10.1128/AEM.00195-20
1251 Mueller RC, Paula FS, Mirza BS, et al (2014) Links between plant and fungal
1252 communities across a deforestation chronosequence in the Amazon rainforest.
1253 ISME J 8:1548–1550. https://doi.org/10.1038/ismej.2013.253
1254 Myers N, Mittermeier RA, Mittermeier CG, et al (2000) Biodiversity hotspots for
1255 conservation priorities. Nature 403:853–558. https://doi.org/10.1038/35002501
1256 Nekola JC, Mcgill BJ (2014) Scale dependency in the functional form of the distance
1257 decay relationship. Ecography (Cop) 37:309–320. https://doi.org/10.1111/j.1600-
1258 0587.2013.00407.x
1259 Nemergut DR, Schmidt SK, Fukami T, et al (2013) Patterns and processes of microbial
1260 community assembly. Microbiol Mol Biol Rev 77:342–356.

1261 https://doi.org/10.1128/MMBR.00051-12
1262 Oksanen J, Blanchet FG, Friendly M, et al (2019) vegan: Community Ecology Package.
1263 R package version 2.5-6. 104
1264 Pärtel M, Öpik M, Moora M, et al (2017) Historical biome distribution and recent
1265 human disturbance shape the diversity of arbuscular mycorrhizal fungi. New
1266 Phytol 227–238. https://doi.org/10.1111/nph.14695
1267 Paula FS, Rodrigues JLM, Zhou J, et al (2014) Land use change alters functional gene
1268 diversity, composition and abundance in Amazon forest soil microbial
1269 communities. Mol Ecol 23:2988–2999. https://doi.org/10.1111/mec.12786
1270 Pedrinho A, Mendes LW, Merloti LF, et al (2019) Forest-to-pasture conversion and
1271 recovery based on assessment of microbial communities in Eastern Amazon
1272 rainforest. FEMS Microbiol Ecol 95:1–10. https://doi.org/10.1093/femsec/fiy236
1273 Pellissier L, Niculita-Hirzel H, Dubuis A, et al (2014) Soil fungal communities of
1274 grasslands are environmentally structured at a regional scale in the Alps. Mol.
1275 Ecol. 23:4274–4290
1276 Poudel R, Jumpponen A, Schlatter DC, et al (2016) Microbiome Networks: A Systems
1277 Framework for Identifying Candidate Microbial Assemblages for Disease
1278 Management. Phytopathology 106:1083–1096. https://doi.org/10.1094/PHYTO-
1279 02-16-0058-FI
1280 Powell JR, Karunaratne S, Campbell CD, et al (2015) Deterministic processes vary
1281 during community assembly for ecologically dissimilar taxa. Nat Commun 6:1–10.
1282 https://doi.org/10.1038/ncomms9444
1283 Powell JR, Rillig MC (2018) Biodiversity of arbuscular mycorrhizal fungi and
1284 ecosystem function. New Phytol 220:1059–1075.
1285 https://doi.org/10.1111/nph.15119
1286 Ranjard L, Dequiedt S, Chemidlin Prévost-Bouré N, et al (2013) Turnover of soil
1287 bacterial diversity driven by wide-scale environmental heterogeneity. Nat Commun
1288 4:1–10. https://doi.org/10.1038/ncomms2431
1289 Reznick D, Bryant MJ, Bashey F (2002) r- and K-selection revisited: The role of
1290 population regulation in life-history evolution. Ecology 83:1509–1520.
1291 https://doi.org/10.1890/0012-9658(2002)083[1509:raksrt]2.0.co;2
1292 Ribeiro MC, Metzger JP, Martensen AC, et al (2009) The Brazilian Atlantic Forest:
1293 How much is left, and how is the remaining forest distributed? Implications for
1294 conservation. Biol Conserv 142:1141–1153.

https://doi.org/10.1016/j.biocon.2009.02.021

Robeson MS, King AJ, Freeman KR, et al (2011) Soil rotifer communities are extremely diverse globally but spatially autocorrelated locally. Proc Natl Acad Sci U S A 108:4406–4410. https://doi.org/10.1073/pnas.1012678108

Rocha FI, Ribeiro TG, Fontes MA, et al (2021) Land-Use System and Forest Floor Explain Prokaryotic Metacommunity Structuring and Spatial Turnover in Amazonian Forest-to-Pasture Conversion Areas. Front Microbiol 12:1–13. https://doi.org/10.3389/fmicb.2021.657508

Rodrigues JLM, Pellizari VH, Mueller R, et al (2013) Conversion of the Amazon rainforest to agriculture results in biotic homogenization of soil bacterial communities. Proc Natl Acad Sci U S A 110:988–993. https://doi.org/10.1073/pnas.1220608110

Rodríguez-Valdecantos G, Manzano M, Sánchez R, et al (2017) Early successional patterns of bacterial communities in soil microcosms reveal changes in bacterial community composition and network architecture, depending on the successional condition. Appl Soil Ecol 120:44–54. https://doi.org/10.1016/j.apsoil.2017.07.015

Schütte UME, Abdo Z, Bent SJ, et al (2008) Advances in the use of terminal restriction fragment length polymorphism (T-RFLP) analysis of 16S rRNA genes to characterize microbial communities. Appl Microbiol Biotechnol 80:365–380. https://doi.org/10.1007/s00253-008-1565-4

Sengupta A, Stegen JC, Neto AAM, Wang Y (2019) Assessing Microbial Community Patterns During Incipient Soil Formation From Basalt. 1–18

Shade A, Dunn RR, Blowes SA, et al (2018) Macroecology to Unite All Life , Large and Small. 1–14

Shi Y, Delgado-Baquerizo M, Li Y, et al (2020) Abundance of kinless hubs within soil microbial networks are associated with high functional potential in agricultural ecosystems. Environ Int 142:105869. https://doi.org/10.1016/j.envint.2020.105869

Soininen J, McDonald R, Hillebrand H (2007) The distance decay of similarity in ecological communities. Ecography (Cop) 30:3–12. https://doi.org/10.1111/j.0906-7590.2007.04817.x

Sparling G, West A (1988) A direct extraction method to estimate soil microbial C: calibration in situ using microbial respiration and 14C labelled cells. Soil Biol Biochem 20:337–343

Sparling GP (1992) Ratio of microbial biomass carbon to soil organic carbon as a

sensitive indicator of changes in soil organic matter. Aust J Soil Res 30:195–207. https://doi.org/10.1071/SR9920195

Steele JA, Countway PD, Xia L, et al (2011) Marine bacterial, archaeal and protistan association networks reveal ecological linkages. ISME J 5:1414–1425. https://doi.org/10.1038/ismej.2011.24

Stegen JC, Lin X, Fredrickson JK, et al (2013) Quantifying community assembly processes and identifying features that impose them. ISME J 7:2069–2079. https://doi.org/10.1038/ismej.2013.93

Székely AJ, Langenheder S (2014) The importance of species sorting differs between habitat generalists and specialists in bacterial communities. FEMS Microbiol Ecol 87:102–112. https://doi.org/10.1111/1574-6941.12195

Team RC (2019) R: A language and environment for statistical computing

Tedesco MJ, Gianello C, Bissani CA, et al (1995) Analysis of soil, plants and other materials. Universidade Federal do Rio Grande do Sul, Porto Alegre

Teixeira PC, Donagemma GK, Fontana A, Teixeira WG (2017) Manual de Métodos de Análise de Solo, 3rd edn. EMBRAPA Solos, Brasília

Tripathi BM, Stegen JC, Kim M, et al (2018) Soil pH mediates the balance between stochastic and deterministic assembly of bacteria. ISME J 12:1072–1083. https://doi.org/10.1038/s41396-018-0082-4

Turner S, Pryer KM, Miao VPW, Palmer JD (1999) Investigating deep phylogenetic relationships among cyanobacteria and plastids by small subunit rRNA sequence analysis. J Eukaryot Microbiol 46:327–338

Ulrich W, Gotelli NJ (2010) Null model analysis of species associations using abundance data. Ecology 91:3384–3397. https://doi.org/10.1890/09-2157.1

Vale MM, Tourinho L, Lorini ML, et al (2018) Endemic birds of the Atlantic Forest: traits, conservation status, and patterns of biodiversity. J F Ornithol 89:193–206. https://doi.org/10.1111/jofo.12256

van der Gast CJ, Gosling P, Tiwari B, Bending GD (2011) Spatial scaling of arbuscular mycorrhizal fungal diversity is affected by farming practice. Environ Microbiol 13:241–9. https://doi.org/10.1111/j.1462-2920.2010.02326.x

van der Heyde M, Ohsowski B, Abbott LK, Hart M (2017) Arbuscular mycorrhizal fungus responses to disturbance are context-dependent. Mycorrhiza 27:431–440. https://doi.org/10.1007/s00572-016-0759-3

van Dorst J, Bissett A, Palmer AS, et al (2014) Community fingerprinting in a

1363 sequencing world. FEMS Microbiol Ecol 89:316–330.
1364 https://doi.org/10.1111/1574-6941.12308
1365 Vega-Avila AD, Gumiere T, Andrade PAMM, et al (2014) Bacterial communities in the
1366 rhizosphere of Vitis vinifera L. cultivated under distinct agricultural practices in
1367 Argentina. Antonie van Leeuwenhoek, Int J Gen Mol Microbiol.
1368 https://doi.org/10.1007/s10482-014-0353-7
1369 Wang J, Shen J, Wu Y, et al (2013) Phylogenetic beta diversity in bacterial assemblages
1370 across ecosystems: deterministic versus stochastic processes. ISME J 7:1310–
1371 1321. https://doi.org/10.1038/ismej.2013.30
1372 Wang L, Han M, Li X, et al (2020) Niche and Neutrality Work Differently in Microbial
1373 Communities in Fluidic and Non-fluidic Ecosystems. Microb Ecol 79:527–538
1374 Wang XB, Lü XT, Yao J, et al (2017) Habitat-specific patterns and drivers of bacterial
1375 β-diversity in China's drylands. ISME J. https://doi.org/10.1038/ismej.2017.11
1376 Weinzettel J, Vačkář D, Medková H (2018) Human footprint in biodiversity hotspots.
1377 Front Ecol Environ 16:447–452. https://doi.org/10.1002/fee.1825
1378 Xue R, Zhao K, Yu X, et al (2021) Deciphering sample size effect on microbial
1379 biogeographic patterns and community assembly processes at centimeter scale.
1380 Soil Biol Biochem 156:108218. https://doi.org/10.1016/j.soilbio.2021.108218
1381 Zhao J, Gao Q, Zhou J, et al (2019) The scale dependence of fungal community
1382 distribution in paddy soil driven by stochastic and deterministic processes. Fungal
1383 Ecol 42:100856. https://doi.org/https://doi.org/10.1016/j.funeco.2019.07.010
1384

1385 **FIGURE LEGENDS**

1386

1387 **Fig. 1** Principal Coordinates Analysis (PCoA) of soil microbial communities across land
1388 uses, in the subtropical Atlantic Forest Biome, Southern Brazil. Plots were generated
1389 using Bray-Curtis distance matrices with 1000 Monte-Carlo permutations. Samples are
1390 colored as follow: forest, green circles; no-till, brown circles; pasture, red circles;
1391 Differences in microbial beta diversities clustering among land-uses were evaluated
1392 through Adonis-PERMANOVA (n = 324 samples; 999 permutations; $P_{ADONIS} < 0.05$).
1393

1394 **Fig. 2** Beta diversity distributions between pairs of microbial communities across seasons
1395 and land uses, in the Brazilian Atlantic Rainforest Biome, Southern Brazil. (a) Forest
1396 winter; (b) Forest summer; (c) No-till winter; (d) No-till summer; (e) Pasture winter, and;
1397 (f) Pasture summer. Histograms show the distribution of observed pairwise Bray-Curtis
1398 dissimilarities (x axis) and the frequency of pairwise beta diversities for each diversity
1399 rank bin (y axis). Probability Kernel densities are represented by the blue lines. Pairwise
1400 distributions were compared through Kruskal-Wallis (chi-square) non-parametric test
1401 with Bonferroni correction. Uppercase letters represent differences between seasons for

the same land use while lowercase letters represent differences among land uses for the same season ($P_{corrected} < 0.05$). The red dashed lines represent the mean beta Bray-Curtis dissimilarity for each set of comparisons (n = 54 samples; 1341 beta pairwise comparisons). β_{BC} – Beta Bray-Curtis dissimilarity.

Fig. 3 Overall SparCC network plots of co-occurrence and co-exclusion between OTUs, following long-term land use change and seasons. Only OTUs with SparCC significant (two-sided pseudo-P < 0.01, 100 bootstrapping random permutations) and correlations with a magnitude of SparCC > 0.6 (positive correlation–blue edges) or SparCC < −0.6 (negative correlation–red edges) were included into the network plots. Each node represents an OTU, based on *Hha*I enzyme T-RFLP fingerprint. The size of each node is proportional to the number of connections (that is, degree), while the color of each node is represented by a gradient of betweenness centrality. Network graphs were built with 'Fruchterman Reingold' design, on Gephi software.

Fig. 4 Habitat microbial specialization across mesoregions. The x and y axes represent the OTUs abundance turnover between regions. The number and the percentage of generalists and specialists for each habitat comparison. The classification of generalists and specialists was performed through the CLAM test function in vegan R package, according to the estimated species relative abundance. The test was applied with arguments of K = 2/3 and P < 0.005, according to the supermajority rule. All the counts were added by 1 to let the marginal OTUs evenly arranged in the plot space.

Fig. 5 The distance-decay relationships among pairs of microbial communities, within neighborhoods from 0.03 to 378 km, for (a) overall communities, (b) generalists and (c) specialists. The x axis represents the distance between pairwise microbial communities (n = 324 samples; 13040 beta pairwise comparisons) and the y axis represents the Bray-Curtis dissimilarity for each pair of microbial communities (black border circles). The red lines represent the fitted GLM exponential models, and the blue lines represent the fitted GLM power-law models. The slopes of distance-decay relationships are significantly higher than zero (P < 0.05).

Fig. 6 Samples fitting to theoretical ecological models, based on Akaike information criterion (AIC) for rank abundance distributions of microbial OTUs, across land uses and seasons, in the subtropical Atlantic Forest Biome, Southern Brazil. (a) Rank abundance models based on corrected AIC value from Poisson distributions using maximum likelihood estimation. The lowest AIC value for each sample represented the best-fitted model for general community's assembly. Best-fitted models were calculated by the general equation AIC = −2log-likelihood + 2 × npar. ZSM (Zero Sum Multinomial) and Broken-stick are null models regarding to theoretical neutral assembly while Preemption and Lognormal are niche-based models regarding to deterministic assembly. (b) Box-plots of distributions of calculated dispersal rates across land uses and seasons showing the median (thick black line), the first quartile (lower box bound), the third quartile (upper box bound) and the range of data values that deviate from the box (vertical black lines). Dispersal rates were compared through Kruskal-Wallis (chi-square) non-parametric test with Bonferroni correction. Uppercase letters represent differences between seasons for the same land use while lowercase letters represent differences among land uses for the same season ($P_{corrected} < 0.05$). Dispersal rates were calculated by Etienne's formula. Values of dispersal are between 0 and 1, where the higher the value the greater the

tendency to migration of members of a local microbial community, as represented by each of the 324 soil samples.

Fig. 7 Pairwise beta diversities distribution and simulated deviation from null expectation. Beta pairwise diversities at (a) local and (b) regional scales. Bar-plots of Bray-Curtis dissimilarities across land uses and seasons showing the mean and the standard deviation (vertical black lines) of observed (dark colors) and simulated (light colors) beta pairwise diversities (10000 simulations). Z-scores at (c) local and (d) regional scales. Box-plots of distributions across land uses and seasons showing the median (thick black line), the first quartile (lower box bound), the third quartile (upper box bound) and the range of data values that deviate from the box (vertical black lines). Horizontal lines separate lower and upper significance thresholds of Z-scores distributions (Z = -2 and +2, respectively; $P < 0.05$). Z-scores were generated under null model method 'swap_count' with 10000 simulations. H_1: observed beta diversity is less or greater than simulated values of beta diversity.

TABLE LEGENDS

Table 1 Overall topological properties of SparCC networks of co-occurrence between OTUs, following long-term land-use change and seasons.

Footnote:

[a]Microbial OTUs with at least one significant ($P < 0.01$) and strong (SparCC > 0.6 or < -0.6) correlation;

[b]Number of connections/correlations obtained by SparCC analysis;

[c]SparCC positive correlation (> 0.6 with $P < 0.01$);

[d]SparCC negative correlation (< -0.6 with $P < 0.01$);

[e]The capability of the nodes to form highly connected communities, that is, a structure with high density of between nodes connections (inferred by Gephi);

[f]A community is defined as a group of nodes densely connected internally (Gephi);

[g]The longest distance between nodes in the network, measured in number of edges (Gephi);

[h]Average network distance between all pair of nodes or the average length of all edges in the network (Gephi);

[i]The average number of connections per node in the network, that is, the node connectivity (Gephi);

[j]How nodes are embedded in their neighborhood and the degree to which they tend to cluster together (Gephi).

Table 2 Relative contribution of geographic distance, abiotic factors, and biotic factors influencing bacterial communities with different niche occupancies at overall, local, and regional scales. We calculated Pearson product-moment correlations from the simple (Mantel test; 1000 permutations; $P < 0.05$) and the controlled effects (partial Mantel test; 1000 permutations; $P < 0.05$). From a set of 64 measured parameters, only non-collinear and significant variables were forward-selected and used in the model. Local and regional microbial communities were selected by the geographic limit for autocorrelation (Moran's I = 97.196 km; $P < 0.05$).

Table 3 Individual factors influencing bacterial communities with different niche occupancies at overall, local, and regional scales. We calculated Pearson product-moment

1501 correlations from the controlled effects ((partial Mantel test; 1000 permutations; $P <$
1502 0.05). Only non-collinear and significant variables were forward-selected and used in the
1503 model. Local and regional microbial communities were selected by the geographic limit
1504 for autocorrelation (Moran's I = 97.196 km; $P < 0.05$).

Figures

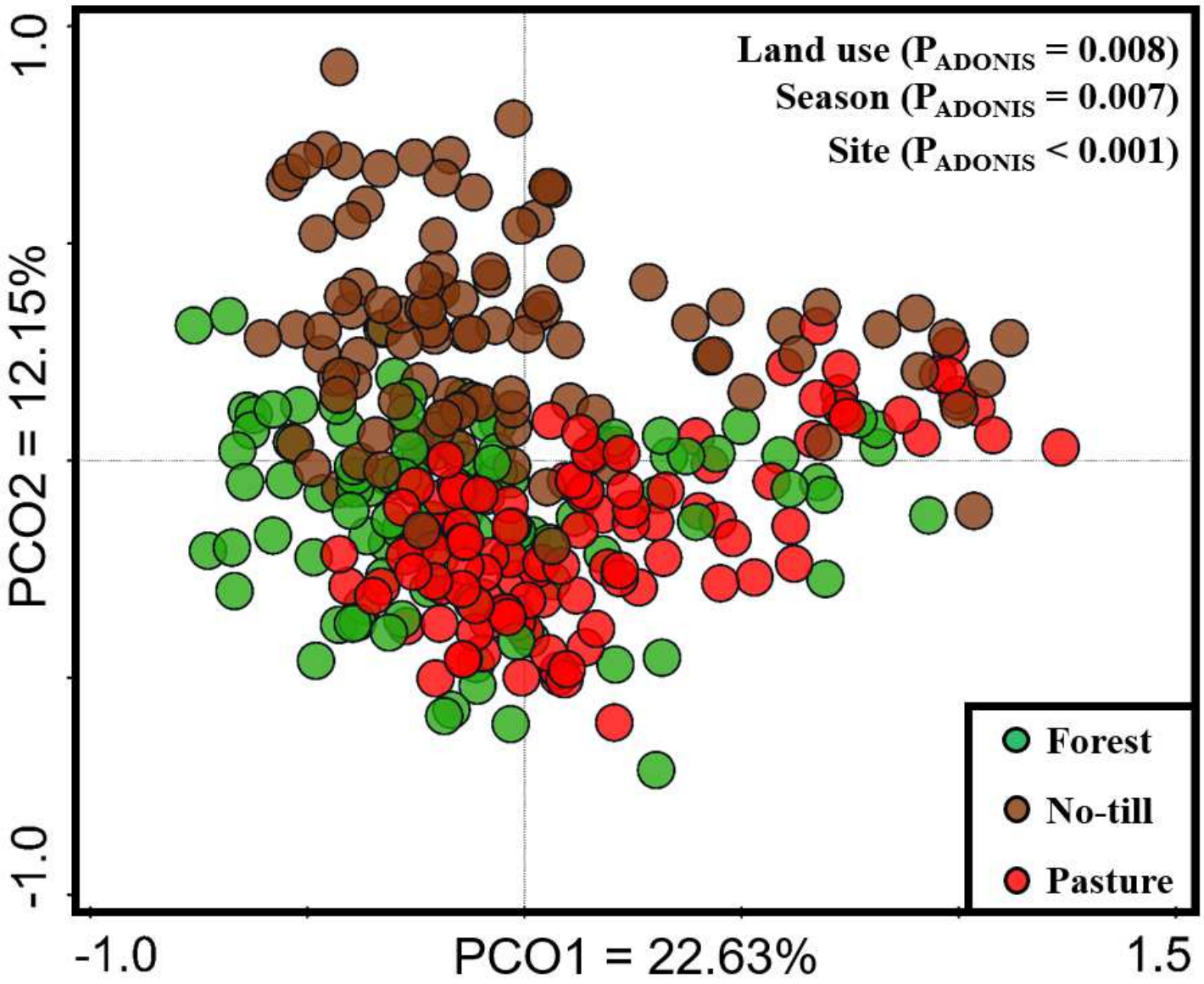

Figure 1

Principal Coordinates Analysis (PCoA) of soil microbial communities across land uses, in the subtropical Atlantic Forest Biome, Southern Brazil. Plots were generated using Bray-Curtis distance matrices with 1000 Monte-Carlo permutations. Samples are colored as follow: forest, green circles; no-till, brown circles; pasture, red circles; Differences in microbial beta diversities clustering among land-uses were evaluated through Adonis-PERMANOVA (n = 324 samples; 999 permutations; $P_{ADONIS} < 0.05$).

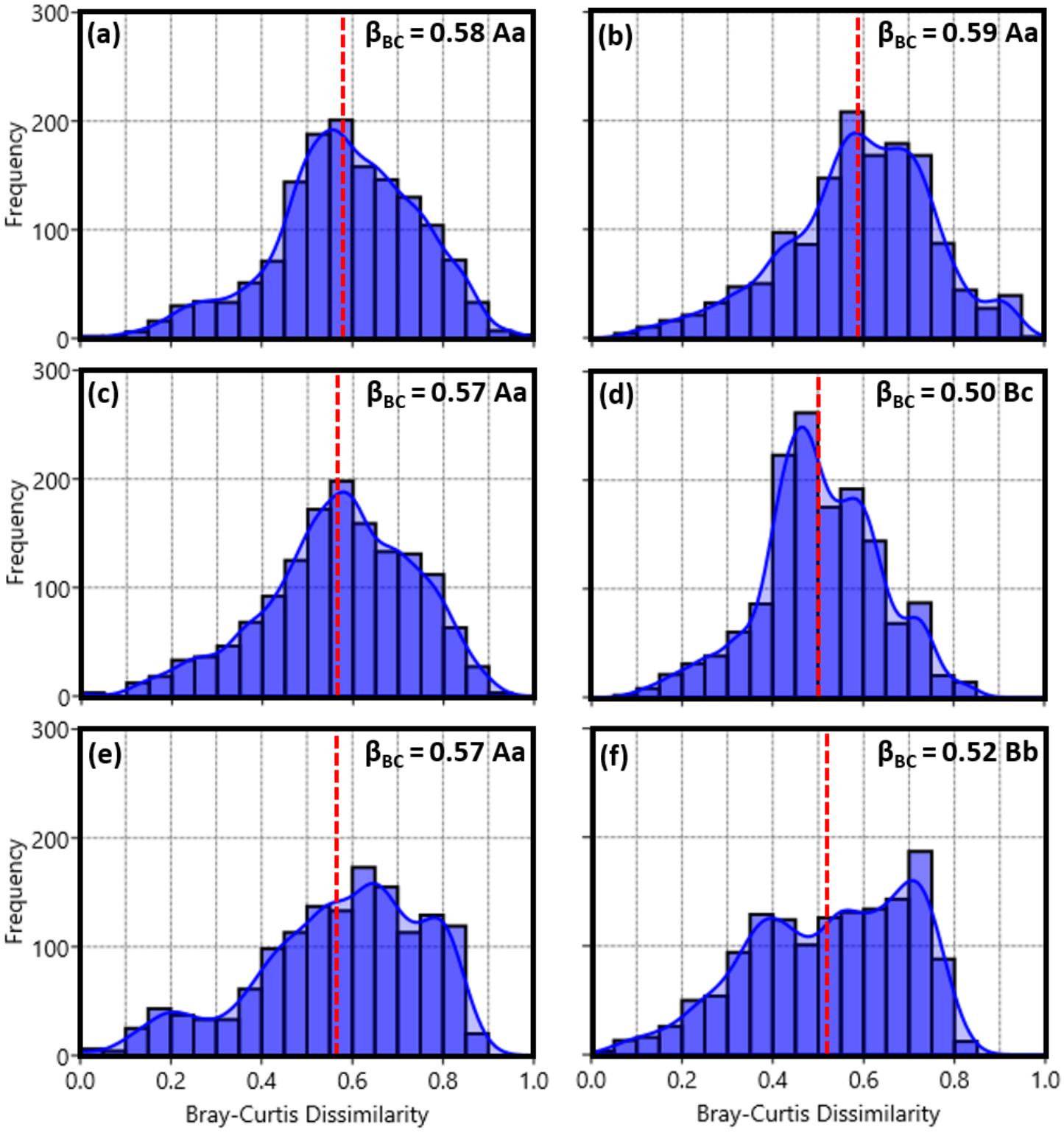

Figure 2

Beta diversity distributions between pairs of microbial communities across seasons and land uses, in the Brazilian Atlantic Rainforest Biome, Southern Brazil. (a) Forest winter; (b) Forest summer; (c) No-till winter; (d) No-till summer; (e) Pasture winter, and; (f) Pasture summer. Histograms show the distribution of observed pairwise Bray-Curtis dissimilarities (x axis) and the frequency of pairwise beta diversities for each diversity rank bin (y axis). Probability Kernel densities are represented by the blue lines. Pairwise

distributions were compared through Kruskal-Wallis (chi-square) non-parametric test with Bonferroni correction. Uppercase letters represent differences between seasons for the same land use while lowercase letters represent differences among land uses for the same season ($P_{corrected} < 0.05$). The red dashed lines represent the mean beta Bray-Curtis dissimilarity for each set of comparisons (n = 54 samples; 1341 beta pairwise comparisons). β_{BC} Beta Bray-Curtis dissimilarity.

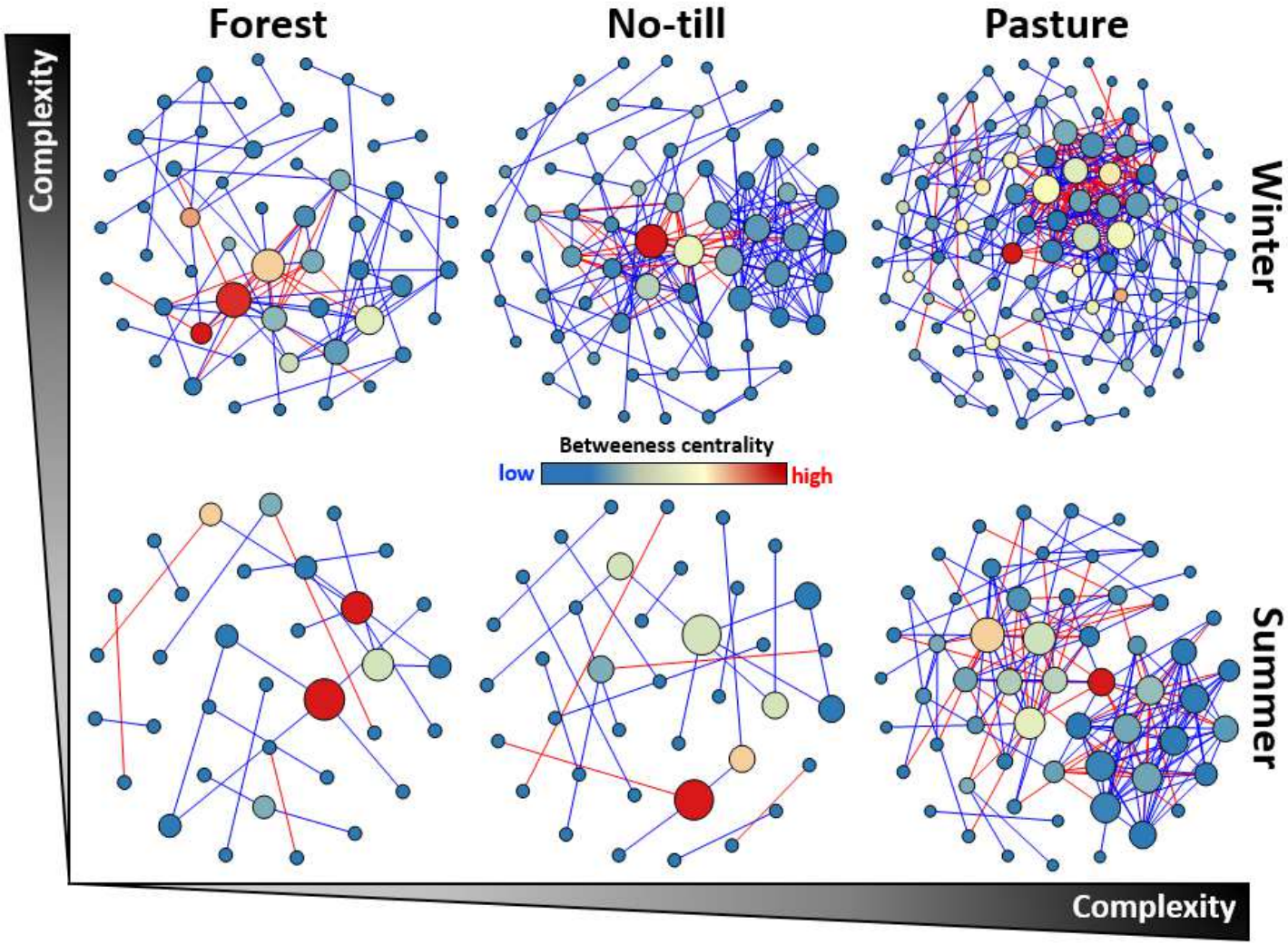

Figure 3

Overall SparCC network plots of co-occurrence and co-exclusion between OTUs, following long-term land use change and seasons. Only OTUs with SparCC significant (two-sided pseudo-P < 0.01, 100 bootstrapping random permutations) and correlations with a magnitude of SparCC > 0.6 (positive correlation–blue edges) or SparCC < −0.6 (negative correlation–red edges) were included into the network plots. Each node represents an OTU, based on *Hha*I enzyme T-RFLP fingerprint. The size of each node is proportional to the number of connections (that is, degree), while the color of each node is represented by a gradient of betweenness centrality. Network graphs were built with 'Fruchterman Reingold' design, on Gephi software.

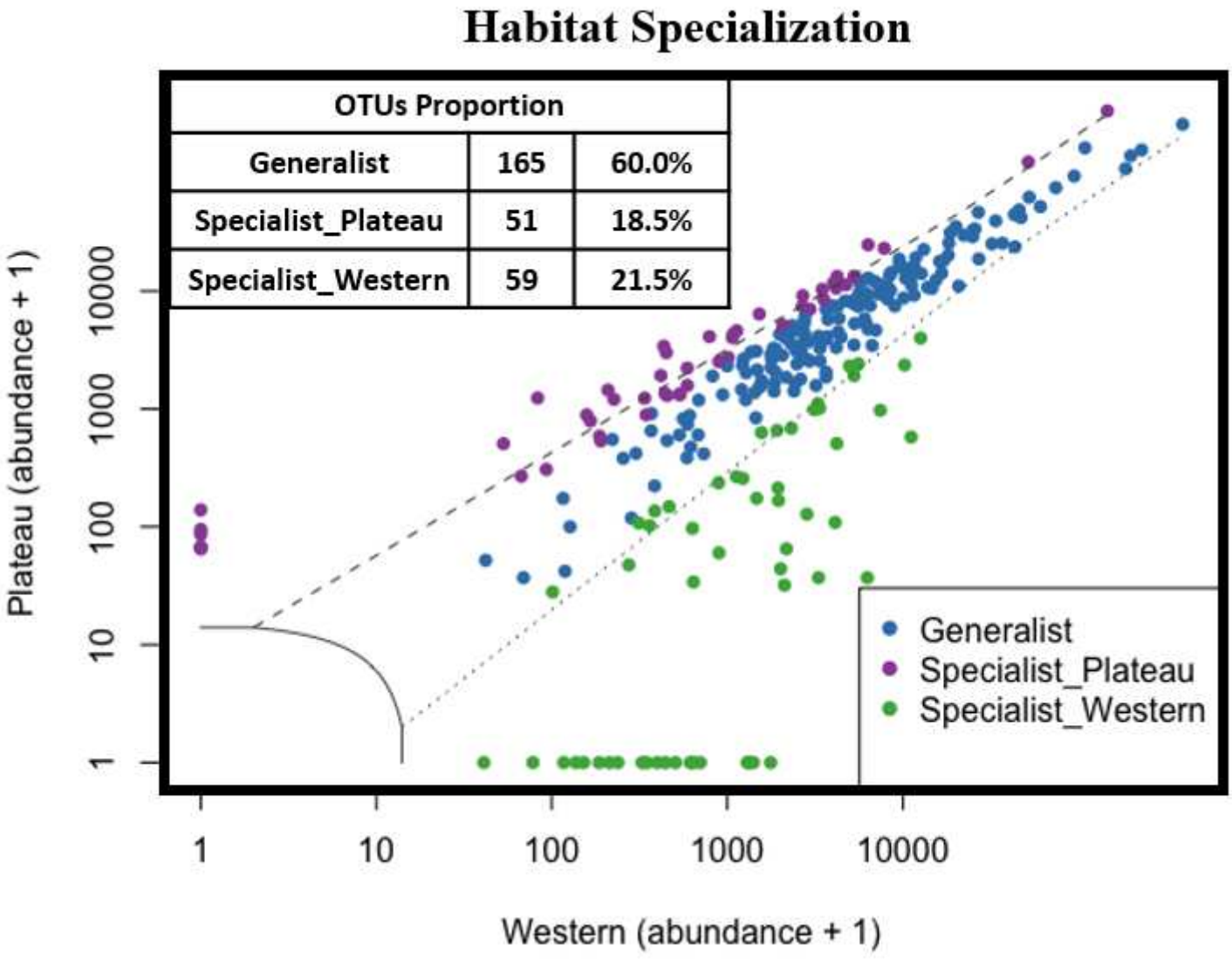

Figure 4

Habitat microbial specialization across mesoregions. The x and y axes represent the OTUs abundance turnover between regions. The number and the percentage of generalists and specialists for each habitat comparison. The classification of generalists and specialists was performed through the CLAM test function in vegan R package, according to the estimated species relative abundance. The test was applied with arguments of K = 2/3 and P < 0.005, according to the supermajority rule. All the counts were added by 1 to let the marginal OTUs evenly arranged in the plot space.

Figure 5

The distance-decay relationships among pairs of microbial communities, within neighborhoods from 0.03 to 378 km, for (a) overall communities, (b) generalists and (c) specialists. The x axis represents the distance between pairwise microbial communities (n = 324 samples; 13040 beta pairwise comparisons)

and the y axis represents the Bray- Curtis dissimilarity for each pair of microbial communities (black border circles). The red lines represent the fitted GLM exponential models, and the blue lines represent the fitted

GLM power-law models. The slopes of distance-decay relationships are significantly higher than zero (P < 0.05).

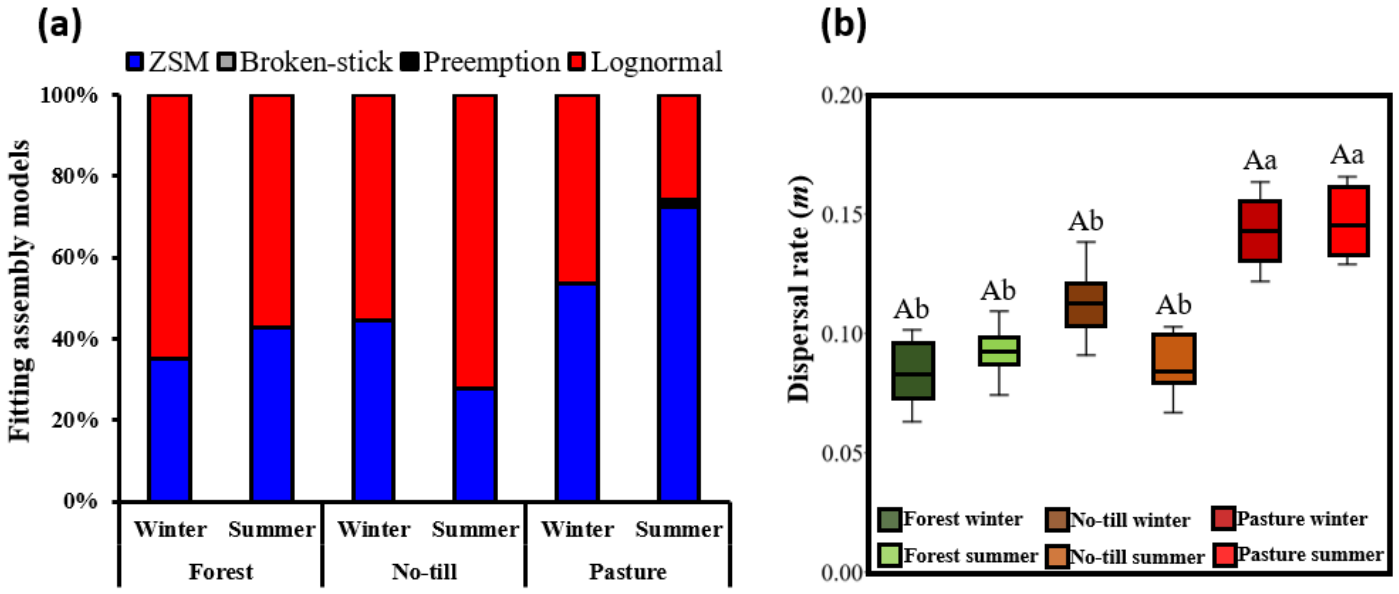

Figure 6

Samples fitting to theoretical ecological models, based on Akaike information criterion (AIC) for rank abundance distributions of microbial OTUs, across land uses and seasons, in the subtropical Atlantic Forest Biome, Southern Brazil. (a) Rank abundance models based on corrected AIC value from Poisson distributions using maximum likelihood estimation. The lowest AIC value for each sample represented the best-fitted model for general community's assembly. Best-fitted models were calculated by the general equation AIC = -2log-likelihood + 2 × npar. ZSM (Zero Sum Multinomial) and Broken-stick are null models regarding to theoretical neutral assembly while Preemption and Lognormal are niche-based models regarding to deterministic assembly. (b) Box plots of distributions of calculated dispersal rates across land uses and seasons showing the median (thick black line), the first quartile (lower box bound), the third quartile (upper box bound) and the range of data values that deviate from the box (vertical black lines). Dispersal rates were compared through Kruskal-Wallis (chi-square) non-parametric test with Bonferroni correction. Uppercase letters represent differences between seasons for the same land use while lowercase letters represent differences among land uses for the same season ($P_{corrected}$ < 0.05). Dispersal rates were calculated by Etienne's formula. Values of dispersal are between 0 and 1, where the higher the value the greater the tendency to migration of members of a local microbial community, as represented by each of the 324 soil samples.

Figure 7

Pairwise beta diversities distribution and simulated deviation from null expectation. Beta pairwise diversities at (a) local and (b) regional scales. Bar-plots of Bray-Curtis dissimilarities across land uses and seasons showing the mean and the standard deviation (vertical black lines) of observed (dark colors) and simulated (light colors) beta pairwise diversities (10000 simulations). Z-scores at (c) local and (d) regional scales. Box-plots of distributions across land uses and seasons showing the median (thick black line), the first quartile (lower box bound), the third quartile (upper box bound) and the range of data values that deviate from the box (vertical black lines). Horizontal lines separate lower and upper significance thresholds of Z-scores distributions (Z = -2 and +2, respectively; $P < 0.05$). Z-scores were generated under null model method 'swap_count' with 10000 simulations. H_1 : observed beta diversity is less or greater than simulated values of beta diversity.

Supplementary Files

This is a list of supplementary files associated with this preprint. Click to download.

- GossSouzaetalsupporting2022v0.pdf